Declaration of Authorship

I hereby confirm that I have written the accompanying thesis by myself, without contributions from any sources other than those cited in the text and acknowledgements.

This applies also to all figures, drawings, maps and images included in the thesis.

Freiberg, 02.09.2022

Dulguun Narmandakh

Acknowledgement

It is a genuine pleasure to get the chance to properly express my sense of thanks and appreciation to every teacher I have had a chance to encounter, my thesis supervisors, and my family for helping me and guiding me throughout my life. Although I have been lucky enough to get many fantastic opportunities, it would have been impossible to grab them without these people.

I would also like to give special thanks to my supervisor, advisor, and friend Dr. Reza Taherdangkoo for the continuous support and understanding of my situation. You are the one who made this project possible, helped me to get the best out of myself, and gave me step-by-step counsel. Thank you, and it was a blessing to work under such a humorous, warm-hearted, yet rightful person.

In addition, thank you to my dear friend Lalropuia, for sharing the long studies and pandemic times and helping me finish my studies smoothly. Thanks to all my friends, specially Egshiglen for understanding and caring for me during the difficult days.

And finally, last but by no means least; I am deeply grateful to my family for their endless love, moral support, and emotional support. Even using every single paper in the world to express my gratitude, I cannot express it enough. You are the ones who made all these possible.

Thanks for all your encouragement!

Abstract

Clay soils can exhibit excessive swelling due to changes in moisture content. The clay swelling and pressure exerted from it threatens the long-term stability of structures and foundations, and thus, a correct understanding and prediction of clay swelling properties is essential in many geotechnical projects. We present feed-forward (FF) and cascade-forward (CF) network models trained with Levenberg–Marquardt (LM) and Bayesian optimisation (BR) algorithms to determine swelling potential of natural and artificial clayey soils. The compiled dataset includes various types of soils covering a wide span of swelling potential, and swelling pressure, ranging from 0.01 to 168.6$\%$, and 25 to 1297.82 kPa, respectively. The activity, moisture content, dry unit weight, liquid limit, plastic limit, plasticity index, gravel content, sand content, silt content and clay content (C) were considered as the input parameters of network models because these are commonly measured during the experimental testing of soil behavior. The developed model showed substantial improvements over previous empirical and semi-empirical correlations in determining the swelling potentials of both natural and artificial soils as well as the swelling pressure.

We employed feed-forward (FFNN) and cascade-forward neural network (CFNN) models trained with Bayesian regularization (BR) and Levenberg–Marquardt (LM) algorithms to determine swelling potential and swelling pressure of clayey soils over a wide range of conditions. A sufficiently large dataset containing free swell experimental data collected from the literature were used to develop the network models. Moreover, the predicted values were compared with different empirical correlations. The FFNN-LM achieved the highest overall accuracy among all network models for both of the output parameters as its predictions showed an acceptable agreement with the experimental data. The model outperforms the tested empirical equations in predicting swelling properties of clayey soil over a span of conditions for which the model was trained.

Contents

List of Figures

List of Tables

Nomenclature

Symbol	Description
ANN	Artificial neural network
ANFIS	Adaptive neuro fuzzy inference system
BLR	Bayesian linear regression
BPM	Bayes point machine
BR	Bayesian regression
BRNN	Bayesian regularization trained neural network
BT	Boosted trees
CFNN	Cascade forward neural network
DENN	Differential evolution optimization trained neural network
DSVM	Deep support vector machine
FFNN	Feed-forward neural network
LM	Levenberg-Marquardt algorithm
LMNN	Levenberg-Marquardt trained neural network
LR	Logistic regression
MLP	Multi layer perceptron
MLR	Multiple linear regression
MRA	Multiple regression analysis
RBF	Radial basis function
RDF	Random forest
SANN	Sequential artificial neural networks
SCG	Scaled Conjugate Gradient
SVM	Support vector machine
SE	Stacking
VE	Voting
MAD	Median absolute deviation
MAE	Mean absolute error
MSE	Mean square error
A	Activity
C	Clay content $(\%)$
CEC	Cation exchange capacity $(\%)$
CG	Coarse-grained fraction ratio $(\%)$
CSF	Clay size fraction $(\%)$
DD	Dry density (Mg/m^3)
FG	Fine-grained fraction ratio $(\%)$
FS	Free-swell $(\%)$
G_s	Specific gravity
K	Coefficient of permeability (cm/s)
w_L	Liquid limit $(\%)$
MDD	Maximum dry density $(\mathrm{kg\,cm^{-1}})$
OMC	Optimum water content $(\%)$
I_P	Plasticity index $(\%)$
w_P	Plastic limit $(\%)$
σ_{max}^{sw}	Swelling pressure (kPa)
S	Smectite content $(\%)$
SL	Shrinkage limit $(\%)$
SSA	Specific surface area $(m^2gm^{-1}$
e_o	Void ratio
γ_d	Dry unit weight $(\mathrm{kN\,m^{-3}})$
w	Moisture content $(\%)$
Ψ_i	Initial suction of a soil (kPa)
ρ_d	Grain density (g/cm^3)
S_{wi}	Degree of water saturation

1 Introduction

Expansive soil is an enigmatic, privately known hazard that is prone to large volume changes associated with a change in the water content. These problematic soils are threatening in many regions around the world and are more prevalent in arid, semi-arid, and drought-prone areas [1]. The soil swelling has caused severe damage to geotechnical structures such as differential settlement, ground heave, and cracking of pavements. Depending on the amplitude of swelling pressure, constructions of different weights and structures receive mild damage and even collapse. Generally, soil expansion causes more economic damage than earthquakes, floods, hurricanes, and tornadoes combined [2], even though it is more manageable to foreknow and avoid. Hence, a thorough understanding of factors affecting the swelling phenomena is essential for planning and designing engineering measures for the problem.

Clay swelling mainly depends upon the intrinsic soil properties, stress conditions, and environmental factors [3]. Soil properties include clay mineralogy, pore water chemistry, soil suction, plasticity, and dry density, which are considered the initial soil state. The term "clay mineral" refers to phyllosilicate minerals, which impart plasticity to clay and would harden when dried or fired [4, 5]. Experimental research has shown that swelling can occur through crystalline and osmotic swelling [6, 7]. Crystalline swelling can occur in all types of clay minerals due to the incorporation of water molecules into the crystal lattice [8]. Osmotic swelling is limited to clay minerals that contain exchangeable interlayer cations [9] and occurs due to differences between the concentration of cations in the interlayer and pore water [9, 4]. Both phenomena create repulsive forces to separate the clay flakes and the silicate layers from each other leading to volumetric expansion [4, 10]. The osmotic process leads to significantly larger volume increases compared to the crystalline swelling [10].

Swelling potential (SP) and swelling pressure (σ_{max}^{sw}) are inevitable parts of expansive soil as all of the expansive-soil issues relate to the two terms. Swelling potential refers to the volumetric expansion percentile of the soil, whereas swelling pressure refers to the pressure induced by expansion. Thus, the swelling pressure has a stronger relationship to potential hazards, i.e. when the vertical pressure exerted by soil expansion is greater than the foundation pressure [11], the surface above/around the expansion bulges and causes damage to what's on it. Affecting factors to the swelling behavior of expansive soil have been studied throughout the research. For instance, McCormack et al. [12] noted that clay content (C) has the capability to make a well-grounded parameter for prediction while on the contrary Gray et al. [13] has the opposite standing: says the C has no relation to the swelling behavior. According to EA [14], initial moisture content, initial dry density, and coarse particle content play a crucial role in defining the swelling pressure of expansive soil. Also, the high importance of the swell index and plasticity index (I_{P}) were found by Parker et al. [15]. Generally, the swelling pressure and swelling potential are dependent on parameters such as cation exchange capacity (CEC), liquid limit (w_{L}), plastic limit (w_{P}), moisture content (w), etc., as well as other physical and chemical factors. The ANN development took all of these into consideration along with the common availability of parameters for experimental studies. Models used activity (A), dry unit weight (γ_{d}), w, w_{L}, w_{P}, I_{P}, C for SP and additional gravel content, sand content, and silt content for σ_{max}^{sw}.

As reported in 1981, more than $2.3 billion worth of damage is inflicted annually due to the shrinking and swelling behavior of expansive soil [16] in the United States, which is estimated to be over $15 billion in later reports [17]. Recently, Zumrawi et al. [18] studied ten randomly chosen buildings that

are built on expansive soils in three regions of Khartoum state. Khartoum state buildings are built on expansive soil and suffer from light damage [19]. Surveyed buildings showed high diversity in terms of construction material, weight, and structure. In their study, they investigated every corner and counted crack, break and heave to find fence and exterior wall cracks, as well as severe internal wall and floor cracks and heaves, repeatedly occurred during the investigation. These cracks and heaves are between 1mm to 100mm wide making the building hazardous to live in. Zumrawi et al. [18] concluded that poor surface drainage, gardens watering close to buildings, sources of water leakage, and improper design of foundations are the main reason for the damages. The initial moisture content of the expansive soil has a significant change in the swelling potential of the soil. Less the initial moisture content, more the swelling potential of the soil. This indicates that drier soil swells more than humid soil with enough water. In the history of Britain, the biggest economic damage infliction related to geohazard was caused by the swell-shrink behavior of expansive soil after the drought in 1947. A total cost of £3 billion was spent during the decade-long hazard [2].

Since the 1970s, countries started to pay attention to the hazard which follows soil expansion [20], and many laboratory experiments have been conducted ever since to measure the swelling behavior of clayey soil. International Society of Rock Mechanics (ISRM) published the first proposal for swelling tests in 1979 and later updates were published later in 1989 and 1999 respectively [21]. Swelling tests operate under two general circumstances (1) without confining conditions and (2) with oedometric confining conditions. The swelling process in both aforementioned tests is initiated through watering the specimen. Depending on the specimen, however, modifications are recommended during specimen preparation. These modifications are suggested in almost every testing norm and standard (e.g. ISRM, DGGT, and VSS). The most common laboratory test methods are oedometer test and free swelling test [21]. The oedometer test is a test process with confining conditions and objectively simulates the one-dimensional field drainage and deformation conditions. It is the most commonly conducted and important test method that is used to measure the vertical displacement of the specimen under controlled vertical load. Free-swell test is a simple procedure with no convoluted tools to indicate the swell of the specimen without constraints that measure the swelling of a specimen under unconfined conditions. The method measures the expansion rate of the soil which is rested under water until the sample attains an equilibrium state. However, a potential problem associated with this test is the disintegration of the specimen during the experiment leading to ambiguous outcomes [21]. Also, these conventional laboratory methods are highly reliable but time-consuming and need expensive laboratory equipment, making them complicated to use consistently for large-scale soil studies.

Originating from the experimental studies, empirical and semi-empirical correlations based on physico chemical processes have been developed to describe the swelling behavior of clayey soils, such as, machine learning (ML) techniques [22] [23], and empirical relationship analysis [24]. The employed techniques generally involved development of empirical correlation formulas before artificial intelligence (AI) developed adequately. These formulas were attempted using soil index properties such as Atterberg limits, clay size fraction, dry density, and moisture content [25, 26, 27, 28, 29], as well as chemical properties and surface area [30, 31]. Such empirical and semi-empirical correlations are very soil specific, and usually provide satisfactory estimations over the specified domain of application. Even though these empirical correlations make convincing estimations on the trained dataset, they lack the generality necessary to cover a broad range of soil types [32] or suffer from important constraints. For instance, they cannot account for the complexities of natural or compacted soils, which is due to their simplifying

assumptions [27, 25].

The rapid development of computer science has introduced a new path for prediction and estimation models. Reliable predictive models that relate the swelling behavior to basic test parameters namely, clay content and Atterberg limits are necessary to determine the swelling potential and pressure of clayey soils: This would avoid the time and effort required for laboratory testing. Recently, ML has been employed to determine the swelling potential and pressure of clayey soils because of its high ability to generate accurate predictive schemes for different complex systems. ML can handle complex nonlinear input-output relationships and a have high interpolation capacity [33]. To describe the swelling behavior of clayey soils, various AI predictive models based on supervised learning can be applied.

Comparative analysis was designed to evaluate the performance of the most accurate network model with experimental data obtained from the literature as well as Nayak et al. [25], Seed et al. [26] and Basma [27] correlations. The Leverage method was employed to examine the dataset quality and define the applicability realm of the model.

1.1 Expansive soil

Any soil or rock mineral which changes in volume in the presence or lack of moisture is considered expansive soil. For swelling of expansive soil, mechanical and chemical swelling mechanisms were observed. The focus of this research is the physical swelling mechanisms, where electrical forces or pore water pressure cause the swelling [34]. Expansive soil varies extensively depending on the composition

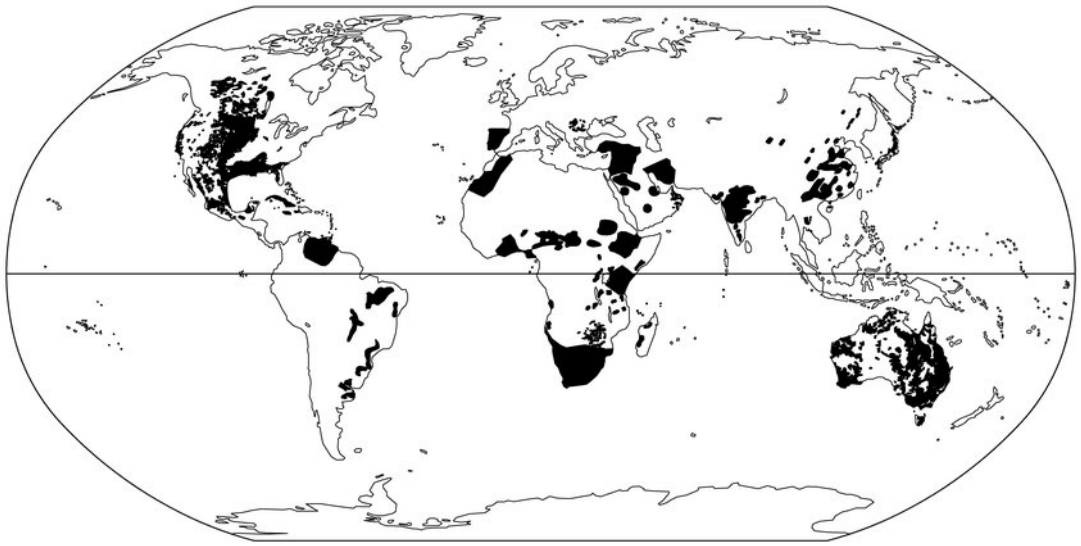

Figure 1: Distribution of expansive soil world-wide, 2015, Nelson et al. [35]

and portion of the expansive minerals. The expansive minerals include clay-based minerals with a positive charge of cations in the interlayer locations. These cations have the ability to adsorb liquid leading to an increase in basal spacing. This adsorption process leads to volumetric expansion for the composition [10]. Several clay-type minerals exist, namely smectite, bentonite, montmorillonite, beidellite, vermiculite, attapulgite, nontronite, illite, and chlorite [36]. Comprehensive locations of the expansive soil are illustrated in Figure 1 according to Nelson et al. [35] reported in 2015.

Sridharan, A. and Prakash, K. [37] proposed an expansive soil classification based on oedometer expan-

sion percent. In this classification, soils are categorized into five classes from negligible to very high expansivity. According to Table 1, when the expansion is over five percent, clay is considered swelling and needs attention. It is studied that even if only 3% of ground swelling occurs under the foundation, it could spoil a structure [1]

Table 1: Expansive soils classification proposition [37]

Oedometer expansion [%]	Clay type	Soil expansivity
<1	Non-swelling	Negligible
1-5	Mixture of swelling and non-swelling	Low
5-15	Swelling	Moderate
15-25	Swelling	High
>25	Swelling	Very high

Not only does the soil type matters when it comes to identifying actual swelling value, but also the environmental factors as well as stress conditions. Previous investigations learned the factors affecting the swell-shrink behaviors of in situ soil. These factors are mainly grouped as follows [3]:

- Soil properties
- Environmental factors
- Stress condition

Soil properties include clay mineralogy, water properties, soil suction, plasticity, and dry density. These properties could be argued as the initial soil state. Clay mineralogy covers clay types (e.g. kaolinite, montmorillonite) and the layer compositions of clay [38]. Water is commonly defined as H_2O and a mixture of other minerals, but the swelling of clay considers more about the cation concentration of the water. Emphasizing two different clay swelling relating to clay hydration is essential: intracrystalline swelling involving the adsorption of limited amounts of water in the interlayer spacing, and osmotic, which is related to unlimited adsorption of water due to the difference between ion concentrations close to the clay surface and the pore water swelling [4].

Soil suction, often referred to as negative pore water pressure, influences the soil's mechanical properties. Experimental studies have shown that the swelling potential decreases with increasing soil suction for all types of soil [39]. Soil suction is linked to the water content of soil. The liquid limit (w_L) and plastic limit (w_P), collectively known as the Atterberg limits [40], and the plasticity index (I_P), are widely known as essential parameters for determining practically relevant water content ranges as well as the swelling potential of soils. The w_L defines the water content at which the soil transitions from a plastic behaviour to a liquid-like consistency [41]. The w_P describes the limit of soil workability, i.e., a kind of ductile-brittle transition [41]. Soils with high w_L and I_P, defined as the difference between the liquid limit and the plastic limit, tend to have higher swelling potential. The swelling potential is also directly related to the dry density of clay-rich soils. A high dry density indicates a closer packing of the particles [42] in the clay material, which results in a higher swelling potential [43].

Environmental factors and soil conditions affect the soil swelling behavior primarily through water infiltration and evaporation, which lead to soil water ingress and egress [44]. Factors affecting the soil environment are initial and current soil suction, water content, climate, groundwater, drainage, vegeta-

tion, permeability, and temperature [3]. The in-situ conditions and the stress history of the soil affect its shrinking and swelling behavior. For instance, a highly consolidated soil is more critical than a normally consolidated soil with a comparable void ratio [45, 44]. An expansive soil would not swell where it is situated below the groundwater level, or subjected to loads higher than or equal to its swelling pressure.

The treatments for the expansive have three basic directions which are soil substitution, soil maintenance, and soil stabilization. Soil substitution and soil maintenance are straightforward approaches that need non-expansive soil substitution instead of former expansive soil and constant moisture application to the ground. However, there have been many studies regarding stabilization. This technique tweaks existing soil to certain standards meeting the needed specifications for lifelong work [46].

1.2 Machine learning

1.2.1 Existing artificial intelligence models - Swelling potential

Several intelligent models have been developed to determine the swelling potential of expansive soils. A summary of the existing AI models is listed in Table 2. Although these models are able to predict the soil swelling indices over the specified domain of application, all of them have some constraints: (1) being valid over a limited range of conditions or (2) the predictions are not sufficiently accurate. Table 2 shows that most of the AI models were developed based on either a relatively small dataset and/or a few input parameters, which limits their generalisation abilities.

For instance, Yilmaz et al. [47] built three different AI models using a dataset containing 215 soil samples with three input parameters (w_{L}, A, CEC). All the models showed a good prediction accuracy for the regression task. But, the authors did not provide any information about the dataset, and the models cannot be reused. Ermias et al. [48] used 160 samples collected from four locations in Ethiopia to build an ANN model based on six input parameters. However, the model had a very limited accuracy in predicting the swelling potential of clay-rich soils. Eyo et al. [49] compiled a relatively large dataset, which was then divided into three subsets, i.e. scenarios, with each scenario considering only three input parameters. All the models build based on scenario 3 (input parameters of A, w_{L}, CEC) provided a satisfactory performance. But, the models built based on the other input parameters, i.e. scenarios 2 and 3, failed in determining the clay soil swelling potential. Erzin et al. [50] built an ANN model and used cross validation technique as stopping criterion. The built model has 58 data points, out of which, 56% were used for training, 24% for testing, and 20% for validation. As for the MRA, SPSS 8.0.0 was used for the development.

1.2.2 Existing artificial intelligence models - Swelling pressure

Estimation models built around AI to estimate the swelling pressure of expansive soils are not rare. The existing models are summarized and illustrated in Table 3. These models mostly gave satisfying statistical results, however, all of them have clear limitations: (1) strictly limited in a range of conditions or (2) not sufficiently accurate. Table 3 shows the small dataset and/or lack of parameters for each of the models; accordingly, models do not satisfy the needs.

For instance, Ashayeri et al. [51] specifically prepared dataset consisted of 35 finer than 4.75mm compacted clay samples covering low to high plasticity to build an FFNN model. The model considered five

Table 2: Intelligent algorithms for the swelling potential of expansive soils.

Algorithm/model	Input parameters	Output paramameters	Data no.	Ref.
FFNN	CSF, w_{L}, I_{P}, e_o, S_{wi}	SP	37	[51]
ANN	γ_d, w, C, CEC, I_{P}	SP	58	[50]
ANFIS	CG, FG, I_{P}, MDD	SP	98	[52]
ANFIS, MLP, RBF	w_{L}, A, CEC	SP	215	[47]
FFNN	C, FG, w_{L}, w_{P}, I_{P}, A	SP	160	[48]
SANN	γ_d, w, e_o, C, I_{P}	SP	40	[53]
BLR, BPM, SVM, DSVM, MLP, LR, RDF, BT, VE, SE	scenario 1 (w, e_o, γ_d) scenario 2 (C, I_{P}, MDD) scenario 3 (A, w_{L}, CEC)	SP	517	[49]
ANN, MRA	C, CEC, I_{P}, γ_d, w	SP	58	[50]

parameters (GSF, w_{L}, I_{P}, e_0, $S_w i$) which made an accurate model. However, the range of parameter values restricted the practical applicability of the model. Similarly, Tahasildar et al. [54] built an ANN model with only around 40 data points and 4 parameters (Ψ_{i}, I_{P}, w, γ_{d}) which showed promising results but failed to account for the soil diversity and had limited generalisation ability.

Das et al. [55] used 230 soil samples collected from laboratory experiments done in Saudi Arabia and Nigeria to develop ANN models trained by three different algorithms (Levenberg-Marquardt, Bayesian regularization, and differential evolution optimization) and SVM. Each model showed acceptable performance while SVM displayed a superior ability to predict swelling pressure. Among the ANN models, the DENN model had the best generalization ability. Following Das et al. [55], Bag et al. [23] used the next largest dataset and the highest number irrespective of their physico-chemical parameters for the model development. The dataset has 185 entries consisted of 14 types of clays and 9 parameters (G_s, SSA, CEC, C, S, DD, w_{L}, and w_{P}). Amidst ANN models trained by LM and SCG, the ANN-LM model reached an acceptable range of prediction with statistically amazing results. However, the MSE of 3.03 (the mean σ_{max}^{sw} of the dataset is 6MPa) which is comparably low in the result is too high to use as a reliable alternative for swelling pressure estimation.

The ANN model built by Ikizler et al. [56], included 8 input parameters (SL, OMC, MDD, K, ρ_{d}, w_{L}, w_{P}, I_{P}) with 103 expansive soil samples. These sample datasets were acquired by artificially mixing two types of soil samples from Turkey and using a special apparatus to modify the sample over almost 52 days. The model has outstanding estimation ability, but it has almost no practicality or generalization ability, as the sample size is negligible if the modification is excluded.

Table 3: Intelligent algorithms for the swelling pressure of expansive soils.

Algorithm/model	Input parameters	Output parameters	Data no.	Ref.
ANN	Ψ_{i}, I_{P}, w, γ_d	$\sigma_{\mathrm{max}}^{\mathrm{sw}}$	∼40	[54]
ANN, MRA	C, CEC, I_{P}, γ_d, w, FS	$\sigma_{\mathrm{max}}^{\mathrm{sw}}$	58	[50]
ANN	ρ_d, w_{L}, w_{P}, I_{P}, SL, OMC, MDD, K	$\sigma_{\mathrm{max}}^{\mathrm{sw}}$	103	[56]
DENN, BRNN, LMNN, SVM	w, γ_d, w_{L}, I_{P}, C	$\sigma_{\mathrm{max}}^{\mathrm{sw}}$	230	[55]
FFNN	CSF, w_{L}, I_{P}, e_o, S_{wi}	$\sigma_{\mathrm{max}}^{\mathrm{sw}}$	35	[51]
ANN (SCG, LM)	G_s, w_{L}, w_{P}, SSA, CEC, C, S, DD	$\sigma_{\mathrm{max}}^{\mathrm{sw}}$	185	[23]

All of the AI models listed in Table 2, and Table 3 are not available to the public, and thus (1) their accuracy and generalization capability cannot be evaluated for other datasets, and (2) they cannot be applied by interested parties for future applications. Therefore, this study aims to provide a rigorous AI-based framework needed for the accurate prediction of the swelling potential of expansive soils for future geotechnical applications.

1.3 Motivation

All the existing ML models developed to determine the clay swelling potential and swelling pressure suffer from intolerable deficiencies. Without reliable estimation technique for the clay swelling potential and swelling pressure, a massive amount of resources are being risked and wasted for laboratory assessment and careless constructions. Therefore, this study presents a robust neural network model to determine the swelling potential and swelling pressure of clayey soils to eliminate the time required for laboratory testing beyond standard index tests. Moreover, the reduced cost and time consumption leverages the geotechnical mapping of expansive soils, i.e Figure 1. The network models were developed using an experimental dataset covering a wide range of conditions using simply attainable physical properties of soil.

1.4 Objectives

In this master's thesis, I aimed to develop genuine predictive models for both swelling potential and swelling pressure of clay related expansive soils. Expansive soil samples and test data were collected and compiled from previous research related to expansive soil. This study did not distinguish between origins of the soil to have broader applicable scale as well as contribution to the geotechnical mapping of expansive soil. The detailed objectives are as follows:

- Researching and collecting experimental data of swelling potential, and swelling pressure of clay-rich soils.
- Analyzing and filtering the dataset based on input parameters to make homogeneous data points suitable for the model.
- Applying different types of ML algorithms available on MATLAB to figure out the best fitting model for the dataset.
- Analyzing, evaluating, and ranking predictive performances of each model.
- Investigating previously developed models and empirical and semi-empirical equations to make a comparative analysis.
- Calculate estimations from empirical and semi-empirical equations.
- Make statistical analysis for outputs of ML, empirical and semi-empirical equations.
- Compare the results from the statistical analysis.

- Pointing out the weak and strong range of input values as well as the source of the dataset which the model works the best for to realize the model.
- Determining and ranking the most important parameters effecting swelling potential and swelling pressure of soil samples.

2 Data

2.1 Data - Swelling potential

We compiled a sufficiently large dataset containing experimental swelling potential data of clay soils. The data are collected from studies that employed the standard soil testing techniques and followed recommended procedures to measure the vertical one-dimensional swelling potential of the soil samples. The compiled dataset has a total of 518 data entries covering a wide range of conditions [57, 58, 59, 60, 51, 61, 62, 63, 64]. The description of the data and ranges of parameter values are presented in Table 4. In some cases, for instance [51], the plasticity index (I_{P}) and plastic limits (w_{P}) of the soil were not provided in the original data, and thus were calculated using the following equation [65]:

$$w_{\mathrm{P}} = I_{\mathrm{P}} - w_{\mathrm{L}} \tag{1}$$

The activity (A) is calculated using the following equation [65] where it is in not reported in the literature.

$$\mathrm{A} = I_{\mathrm{P}}/\mathrm{C} \tag{2}$$

where w_{L} is the liquid limit. The Activity (A), moisture content (w), dry unit weight (γ_d), liquid limit (w_{L}), plastic limit (w_{P}), plasticity index (I_{P}), and clay content (C) were considered as the input parameters of the network models because of their potential influence on the soil swelling. These parameters are commonly measured during the experimental testing of soil behavior. Various statistical indices were used to analyse the compiled dataset (Table 5, Figure 2, Figure 3). The dataset includes various type of soils covering a wide span of swelling potential, ranging from 0.01 to 168.6%. Note that most of the soil samples have relatively low to medium swelling potential. Additionally, the dataset has a broad coverage of the soil's plasticity properties. The statistical analysis of the input and output data in terms of histogram and violin plots is depicted in Figure 2 and Figure 3. According to Figure 3, mean value of all the parameters lies close to median indicating that the data distribution is more or less symmetrical. Besides, the high concentration of data is more in the low value range as median and lower quartile are situated next to each other. However, the median, upper quartile and q(0.99) are distant to each other, showing the scarcity of the data in high value range. If we look at parameters individually, A, w_{L}, I_{P}, and SP have high concentration at low values. Hence, the data collected for the study covers clay with low values on these parameters.

The Clay Size Fraction (CSF) which is the percent of material finer than $2\,\mu\mathrm{m}$, obtained from hydrometer analyses is defined as clay content in the study.

2.2 Data - Swelling pressure

Five different research studies [64, 63, 11, 66, 67] are covered in data collection. Swelling pressure data collection is intentionally focused on natural clay and more parameters which reduced scope of the search. Hence, total number of data is 266, much lower than swelling potential data but has stronger concern on naturally formed soil. The input parameters in the collection are gravel content, sand content, silt content, A, C, w_{L}, w_{P}, I_{P}, γ_d, and w. Compared to input parameters used for swelling potential, the

Table 4: Description of the compiled dataset.

Description	Samples	A	w / %	γ_d / kN m^{-3}	w_L / %	w_P / %	I_P / %	C / %	SP / %	Ref.
Natural clay	37	0.38-1.34	7.9-24	14.5-19.6	28-76	20-29	8-50	21-38	3.2-34.4	[51]
Natural clay	78	0.73-0.98	15-40	11.5-17	66-75	21-28	38-54	50-55	0.5-22.1	[61]
Kaolinite and Bentonite mixture	58	0.5-1.5	10-27.7	14-17.9	48-108	25-26	23-82	50.4-54.8	5.3-92.8	[62]
Natural and artificial clay	10	0.6-90	10	16.4	48-255	20-30	28-225	2.5-48	26.2-168.6	[60]
Natural clay	25	1.48-2.02	10.9-15.4	18.3-18.9	69-94	26-48	38-54	20.1-35.7	18.8-34.2	[63]
Natural clay	40	0.61-1.04	1.1-14	10.8-15.9	34-83	14-41	14-57	22-68.5	0.5-47.4	[59]
Natural clay	49	1.5-3.5	18.2-44.6	12.52-16	47-128	22-40	7-89.7	7-89.7	11-64	[57]
Natural clay (subgrade)	20	0.3-1.9	9.4-40.3	12.4-19.6	34-104	17-38	13-68	13-82	0.01-12.7	[58]
Natural clay	201	0.8-3.6	0-20	10-18	60.5-148	17-26	36-131	36-88	0.14-51.6	[64]

Table 5: Statistical evaluation of the input and output parameter values based on 518 entries for swelling potential.

Parameter	Unit	Min.	Max.	Mean	STD	Kurtosis	Skewness
Swelling potential (SP)	%	0.01	168.6	19.79	20.62	12.72	2.98
Activity (A)	-	0.34	90	2.05	7.46	86.12	9.00
Water content (w)	%	0	44.6	15.46	9.81	-0.32	0.43
Dry unit weight (γ_d)	kN m^{-3}	10	19.62	15.03	2.2	-0.53	-0.16
Liquid limit (w_L)	%	28	255	78.42	28.28	5.33	1.66
Plastic limit (w_P)	%	14	48	24.62	5.03	2.3	1.1
Plasticity index (I_P)	%	7	225	53.8	29.14	4.59	1.74
Clay content (C)	%	2.5	88	47.74	17.42	0.75	0.29

swelling pressure has more input parameters which has more concern on size distribution of the soil. The value ranges of data are shown in Table 6. For some instances where parameters are lacking, Equation 1 and Equation 2 are employed to calculate. Also, GRABIT, a MATLAB software, [68] was utilized to convert graphical data to numerical data where the data is provided as graphs, for instance, Rao et al. [64].

Statistical approaches [Figure 5, Figure 4, Table 7] which are identical to the ones used in swelling potential were taken to analyze the compiled dataset. The dataset covers swelling pressure between 25kPa and 1297.82kPa. The negative skewness values are observed in only silt content and γ_d. It shows that the distribution of the data has higher concentration on the lower values than individual mean of each parameters. Also, Figure 5 and Figure 4 show that the better distribution of the dataset in histogram and violin plot respectively.

Table 6: Description of compiled dataset for swelling pressure

Data no.	A	$w(\%)$	γ_d(kN m^{-3})	$w_L(\%)$	$w_P(\%)$	$I_P(\%)$	Gravel(%)	Sand(%)	Silt(%)	C(%)	$\sigma^{sw}_{max}(\%)$	Ref.
185	0.78-3.64	0-20	10-18	60.5-148	17-26	36-131	0	0-34	12.00-48	36-88	33.87561-700.88	[64]
25	1.48-2.02	10.93-15.47	17.95-18.54	69.94	26-48	38-54	2.41-3.97	5.45-9.93	53.4-69.1	20.1-35.7	281.21-442.33	[63]
5	0.56-0.79	25-33	13.64-18.34	64-75	31-43	29-34	6-10.5	13.1-28	17-33.4	43-55	250-960	[66]
36	0.64-1.03	24.2-36	19.42-20.21	52-93	23-33	28-61	0	2.0-33	23-46	40-70	63-1064	[67]

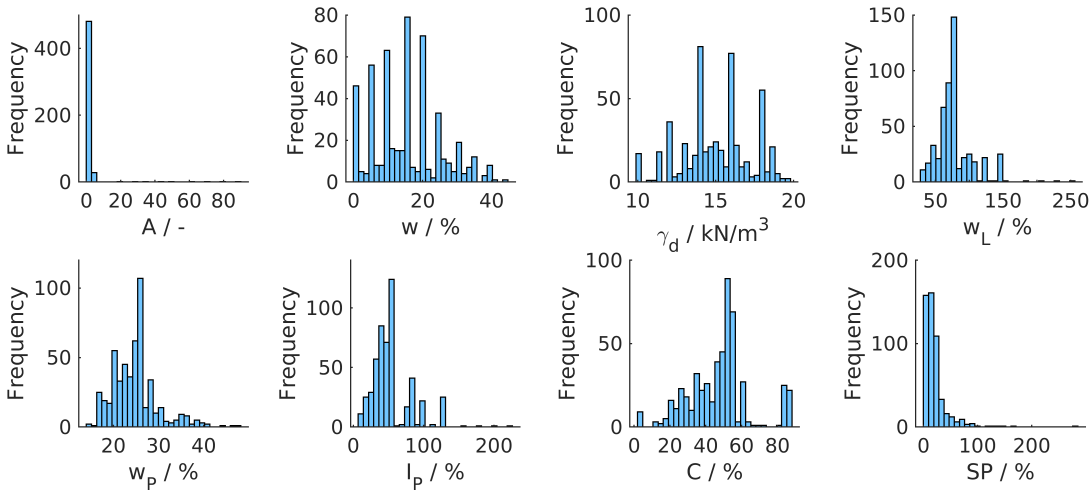

Figure 2: Distribution of the input and output parameters of SP data.

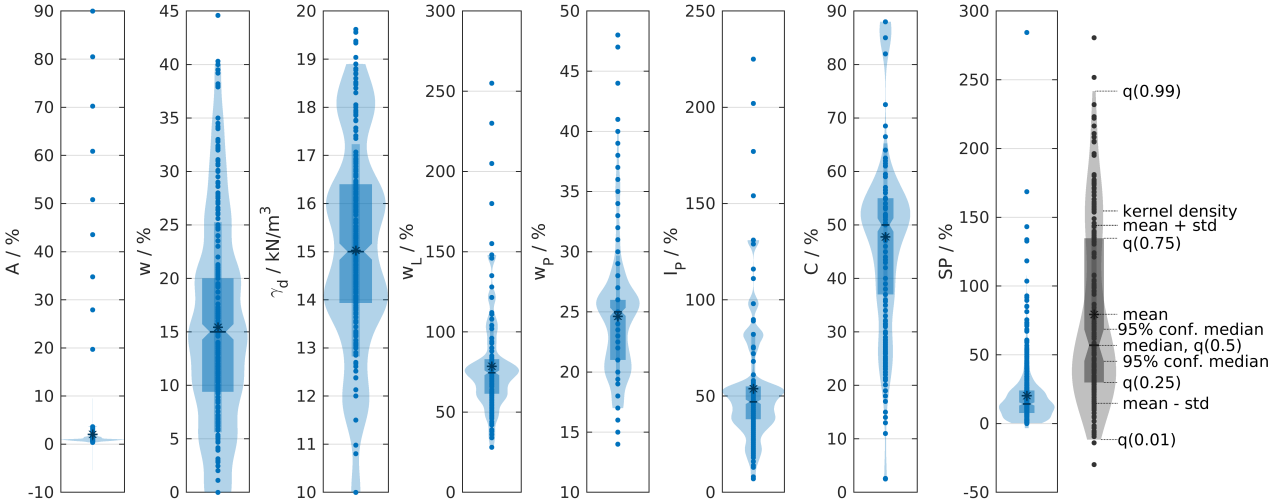

Figure 3: The violin plots of the input and output parameters of SP data.

Table 7: Statistical evaluation of the input and output parameter values based on 251 entries for swelling pressure

Parameter	Unit	Min.	Max.	Mean	STD	Kurtosis	Skewness
Swelling pressure ($\sigma_{\max}^{sw}$)	kPa	33.88	1297.82	289.9	199.0	2.54	1.42
Activity (A)	-	0.56	3.64	1.29	0.83	3.38	2.13
Gravel	%	0.00	10.50	0.50	1.55	17.83	3.92
Sand	%	0.00	34.00	10.38	8.66	1.47	1.23
Silt	%	12.00	69.10	36.59	14.58	-0.42	-0.14
Clay (C)	%	20.10	88.00	52.57	17.61	-0.10	0.71
Liquid Limit (w_L)	%	52.00	148.00	87.31	26.39	0.34	1.12
Plastic limit (w_P)	%	17.00	48.00	24.28	5.86	2.13	1.31
Plasticity index (I_P)	%	28.00	131.00	63.04	29.00	0.44	1.21
Dry unit weight (γ_d)	kN m^{-3}	10.00	20.21	16.15	2.61	-0.88	-0.36
Moisture content (w)	%	0.00	33.00	12.80	8.37	-.99	0.07

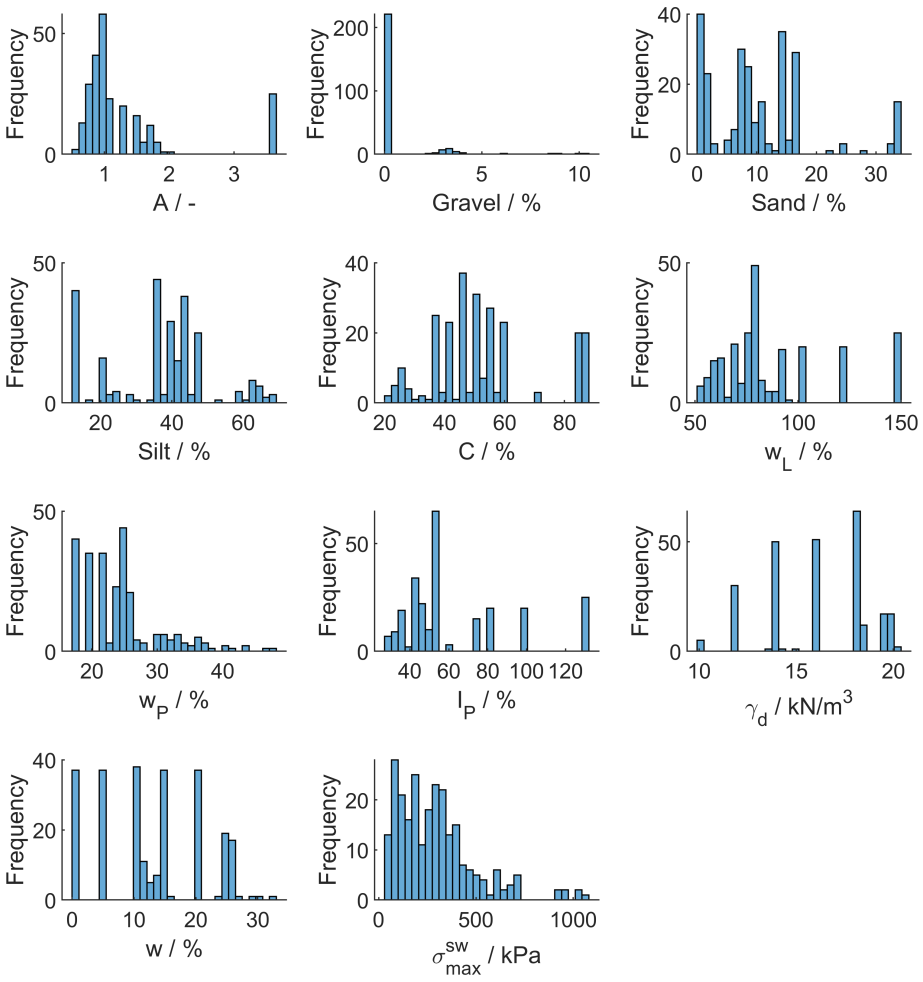

Figure 4: Distribution of the input and output parameters of $\sigma_{max}^{sw} data$.

3 Methodology

3.1 Network models

3.1.1 Feed-forward neural network

A FFNN has a structure that makes it a universal function approximator [69]. A FFNN with a single hidden layer having a finite number of neurons, i.e., nodes, with any continuous sigmoidal nonlinear activation function is capable of approximating any continuous function. The structure of an FFNN consists of several neurons arranged on a layer-by-layer basis, and the connections between the nodes do not form a cycle [70, 71]. A node of an FFNN process information coming through the connection weights. The FFNN can be written as [72, 73]

$$y = f^{\mathrm{o}}(\beta + \sum_{\mathrm{j}=1}^{\mathrm{k}} w_{\mathrm{j}}^{\mathrm{o}} f^{\mathrm{h}}(\beta_{\mathrm{j}} + \sum_{\mathrm{i}=1}^{\mathrm{n}} w_{\mathrm{ji}}^{\mathrm{h}} x_{\mathrm{i}})) \tag{3}$$

where y is the output node, k is the number of nodes in the hidden layer, and n is the number of inputs x_{i}. f^{o} and f^{h} are the activation functions on output and hidden layers, respectively. $w_{\mathrm{j}}^{\mathrm{o}}$ is weight from the hidden layer to output layer, while $w_{\mathrm{ji}}^{\mathrm{h}}$ is the input to hidden layer. β is the weight from bias to output and β_{j} is the weight from bias to hidden layers.

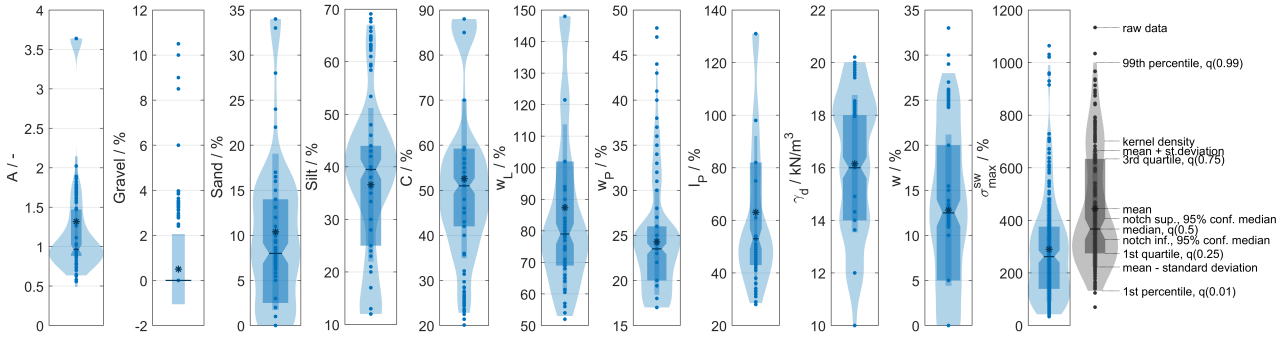

Figure 5: The violin plots of the input and output parameters $\sigma_{max}^{sw} data$.

3.1.2 Cascade-forward neural network

CFNN has a similar structure to FFNN with an additional a weight connection for linking nodes of different layers. The cascade shape allows creating junctions between nodes of a hidden layer with every previous layer. The topology of CFNN brings supplementary flexibility for handling complicated systems with large amount of input data [74, 75]. The CFNN reads as [72, 73]

$$y = \sum_{\mathrm{i}=1}^{\mathrm{n}} f^{\mathrm{i}} w_{\mathrm{i}}^{\mathrm{i}} x_{\mathrm{i}} + f^{\mathrm{o}}(\beta + \sum_{\mathrm{j}=1}^{\mathrm{k}} w_{\mathrm{j}}^{\mathrm{o}} f^{\mathrm{h}}(\beta_{\mathrm{j}} + \sum_{\mathrm{i}=1}^{\mathrm{n}} w_{\mathrm{ji}}^{\mathrm{h}} x_{\mathrm{i}})) \tag{4}$$

where f^i is the activation function from the input layer to the output layer and w_i^i is weight from the input layer to the output layer. Both FFNN and CFNN algorithms for SP were implemented in MATLAB 2021b while FFNN and CFNN for $\sigma_{\mathrm{max}}^{\mathrm{sw}}$ were performed in MATLAB 2022a.

3.1.3 Network training

We employed the Levenberg–Marquardt (LM) and Bayesian regularization (BR) algorithms to optimize the weights and bias of network models because of their proven abilities in obtaining lower mean squared errors for functioning approximation problems [76, 77, 78]. The LM algorithm is a combination of two minimization methods: the steepest descent and the Gauss-Newton. The LM acts as the steepest descent method when the current solution is far away from the optimal value, and becomes the Gauss-Newton method when the current solution is close to the optimal value [79]. The LM is more robust than the Gauss-Newton method and converges faster comparing to either the Gauss-Newton or gradient descent [78, 79].

Bayesian regularization is an improved version of the LM with some modifications in the calculation procedure [76, 78]. The objective function, aimed to be minimized, is formulated to a weighted summation of squared errors and weights. The coefficients of this function are determined on the basis of Bayesian theorem. BR reduces the overfitting potential in the training process, while eliminating the need for the validation process [77, 71].

Following the ratio of 80:20, the input dataset was randomly divided into training and testing subsets. A sample of 290 data points was used to train the models, while the remaining 72 points were used for the performance evaluation. We used logistic sigmoid activation function in the implementation of

the network models. We used trial and error technique to select the optimum number of neurons in the hidden layer. The number of hidden neurons were varied between 1 to 25. We ran each algorithm five times to ensure the the optimal model was obtained. The performance of the models was evaluated using different statistical indices, including the coefficient of determination (R^2), mean squared error (MSE), mean absolute error (MAE), and mean absolute deviation (MAD) [71].

3.1.4 Leverage statistical method

We employed a leverage statistical approach to evaluate the accuracy of the compiled dataset and identify the application realm of the network models. The implementation procedure of the Leverage approach [80] consists of calculating the model's standardized residuals (SR), the hat matrix, and sketching the Williams plot. The standardized residuals represent deviations of predictions from experimental values. The hat values are the diagonal elements of the hat matrix indicating high leverage data points [81, 82]. The hat matrix H can be written as follows [83]:

$$\mathrm{H} = \mathrm{X}(\mathrm{X}^{\mathrm{T}}\mathrm{X})^{-1}\mathrm{X}^{\mathrm{T}} \tag{5}$$

where X is an $n \times k$ matrix, n is the number of data points, k is the model parameters, and X^{T} is the transposed of the matrix X. The critical leverage value H^* equals $3n/(p+1)$, where p is the number of input parameters of the model. The data points within ± 3 standardized residuals are accepted to cover 99% of normally distributed data [84].

3.2 Empirical and semi-empirical correlations of swelling potential

Many correlations have been developed to estimate soil properties in a simple and systematic manner. These correlations, mostly developed for specific soil types, lack generalisability and are unable to estimate the clay swelling potential in a wide ranges of conditions. The performance of the most accurate network model was compared with Basma [27], Nayak et al. [25], and Seed et al. [26]. Each correlation is briefly described in the following.

Basma [27] developed an empirical correlation based on 128 soil samples collected from Central America and northern Jordan. The swelling potential is calculated as follows [61]

$$\mathrm{SP} = 0.00064\, {I_{\mathrm{P}}}^{1.37}\mathrm{C}^{1.37} \tag{6}$$

Nayak et al. [25] developed a semi-empirical approach to model the swelling behaviour of compacted soils based on the diffuse double layer theory and modified the model by introducing empirical constants obtained from experiments conducted on soil samples covering a wide range of clay content and consistency limits. The swelling potential of kaolinite and bentonite clay minerals can be calculated as

$$\mathrm{SP} = 4.4938 \cdot 10^{-3} {I_{\mathrm{P}}}^{1.74} \frac{\mathrm{C}}{w} + 14.722 \tag{7}$$

The following equation can be used for all types of compacted soils

$$\text{SP} = 2.29 \cdot 10^{-2} {I_\text{P}}^{1.45} \frac{\text{C}}{w} + 6.38 \tag{8}$$

Seed et al. [26] conducted extensive experiments on artificially prepared compacted soils to develop an empirical correlation for the swelling potential of soils, which is expressed as:

$$\text{SP} = K \cdot \text{A}^{2.44} \text{C}^{3.44} \tag{9}$$

where $K \approx 3.6 \cdot 10^{-5}$ is a constant for all types of clay mineral. Seed et al. [26] reported that I_P is the single best parameter to determine the swelling potential of soils and suggested the following correlation, which is most suitable for practical purposes [25, 26].

$$\text{SP} = K \cdot M \cdot {I_\text{P}}^{2.44} \tag{10}$$

where M is a constant, which is equal to 60 for natural soils and 100 for artificial soils [32]. The accuracy loss for using Equation 10 instead of Equation 9 is less than 33% for natural soils with clay contents ranging from 8 to 65% [25, 26].

3.3 Empirical and semi-empirical correlations of swelling pressure

Abiddin Erguler et al. [85] attempted to develop empirical equations based on many parameters (w_L, w_P, I_P, C, Clay-XRAY, FS, MFSI, MBV, CEC, w_{max24}, w_{max72}, w, smectite content). These individual parameters were coupled with clay data from different situations and testing such as SWUD (Swelling pressure of undisturbed sample), SWR (Swelling pressure of remolded sample), SPUD (Swelling percent of undisturbed sample) , SPR (Swelling percent of remolded sample), FS (Free swell), MFSI (Modified free swell index). Among the derived equations from combination of these, the following equation fits the collected dataset of the study:

$$\sigma_{\text{max}}^{\text{sw}} = -227.27 + 2.14 \cdot w + 1.54 \cdot w_\text{L} + 72.49 \cdot \gamma_d \tag{11}$$

where the $\sigma_{\text{max}}^{\text{sw}}$ is in g/cm^2, and γ_d is in g/cm^3 Cantillo et al. [86] strived to develop Atterberg limit and moisture content based empirical equations. However, they did not see particular statistical significance in their study. Then they proposed following equations:

$$\sigma_{\text{max}}^{\text{sw}} = 1460.79 - 397.30 \cdot \ln(w) \tag{12}$$

$$\ln(\sigma_{\text{max}}^{\text{sw}}) = 7.97 - 0.12 \cdot w \tag{13}$$

where the estimation of swelling pressure is calculated with sole dependency on w.

Wu et al. [87] made four different linear relationship and power function analysis with initial water content and moisture content to create following equations with a regression analysis:

$$\ln(\sigma_{\text{max}}^{\text{sw}}) = 765.17 \cdot e^{-14.15w} \tag{14}$$

$$\ln(\sigma_{\text{max}}^{\text{sw}}) = 1.349 \cdot w^{-2} \tag{15}$$

Nayak et al. [25] also developed swelling pressure prediction models for all types of soils as shown in the following equation:

$$\sigma_{\text{max}}^{\text{sw}} = (3.5817 \cdot 10^{-2}) I_{\text{P}} \frac{C^2}{w^2} + 3.7912 \tag{16}$$

4 Results

4.1 Results - Swelling potential

We employed FF and CF networks having one hidden layer, which has shown to be sufficient for various regression tasks [88, 71]. Figure 6 shows the mean squared error for the training and testing phases of different network structures. As an example, the error associated with the FFNN-LM model followed an overall decreasing trend with increasing the number of neurons in the hidden layer until the number of neurons reached its optimal value, i.e. 19 neurons. Then, the error experienced an upward trend with increasing the number of neurons, which is a sign of overfitting. Therefore, the FFNN-LM model having 12 neurons in the hidden layer was selected as the optimal structure due to its lowest MSE value obtained during the testing process. The FFNN-BR network has 22 neurons in the hidden layer, and the CFNN-LM and CFNN-BR networks have 8 and 39 hidden neurons, respectively.

Regression plots of predicted swelling potential values versus experimental values depicted in Figure 7, Figure 8, Figure 9, and Figure 10 show accumulations of the data points close to the unit slope line in both train and test phases for all the models. The statistical analysis, presented in Table 8, shows that the network models yield acceptable accuracy indicted by small MSE values. The FFNN-LM is the most accurate model for predicting the swelling potential having the R^2 value of 0.937, and the MSE, MAE, and MAD values of 43.85, 5.27, 15.32, respectively. Among all the NN models, the CFNN-LM exhibited the lowest predictive ability having a MSE value of 58.65. The developed network models follow the accuracy ranking as FFNN-LM, FFNN-BR, CFNN-BR, and CFNN-LM under the given conditions.

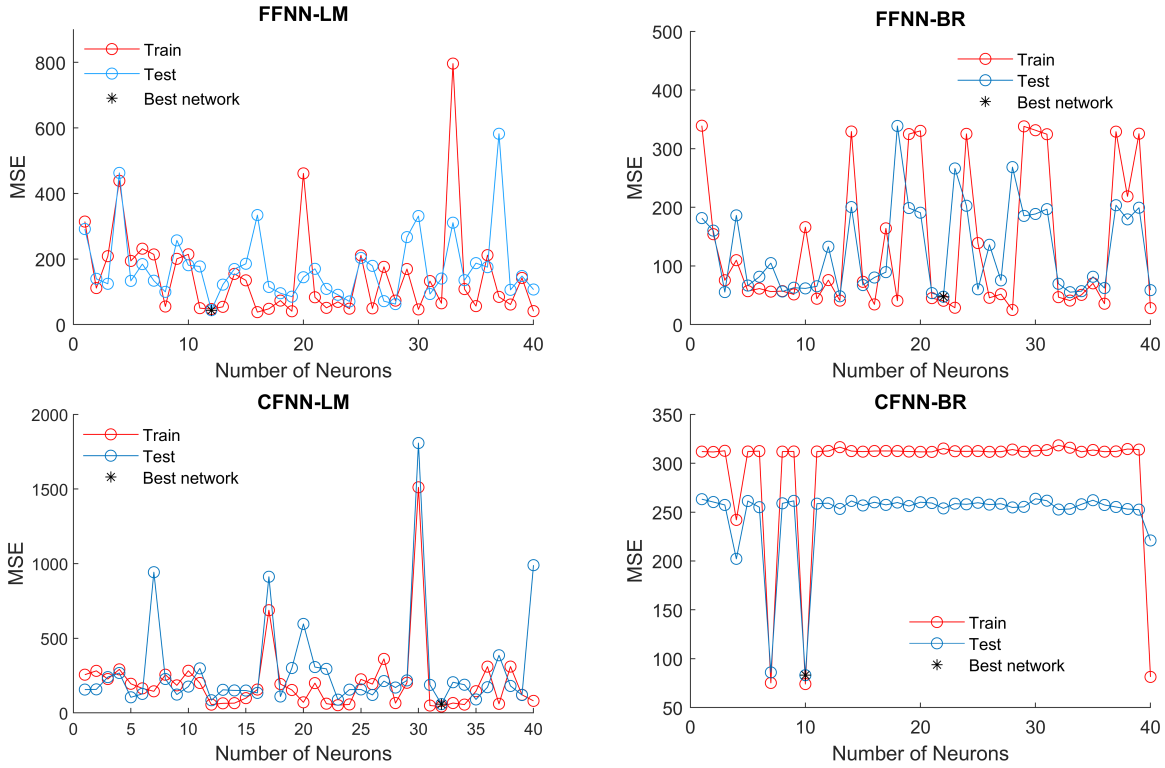

Figure 6: Identifying the optimum number of hidden neurons of all neural network's structures for SP.

The quality of the model predictions is further illustrated in Figure 11, where all the experimental and predicted values are compared to each other. The results show a good agreement between the outputs of the FFNN-LM model and the experimental values. The other models also performed well in predicting

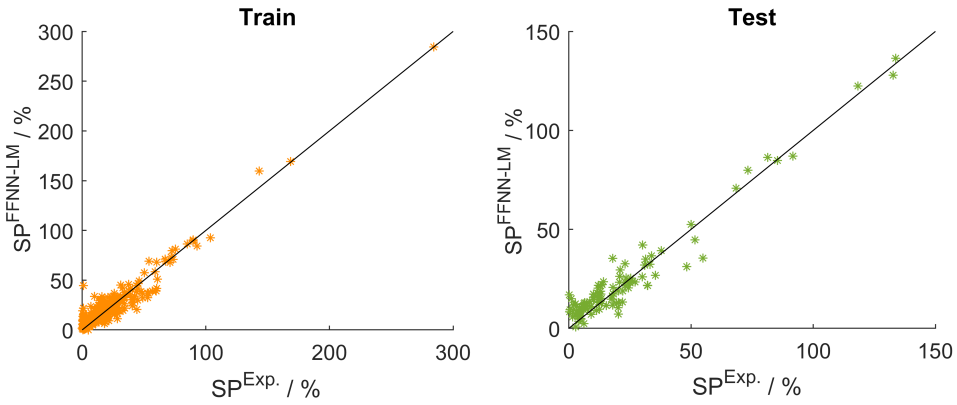

Figure 7: Regression plots of the FFNN-LM model predicted values versus experimental values for SP

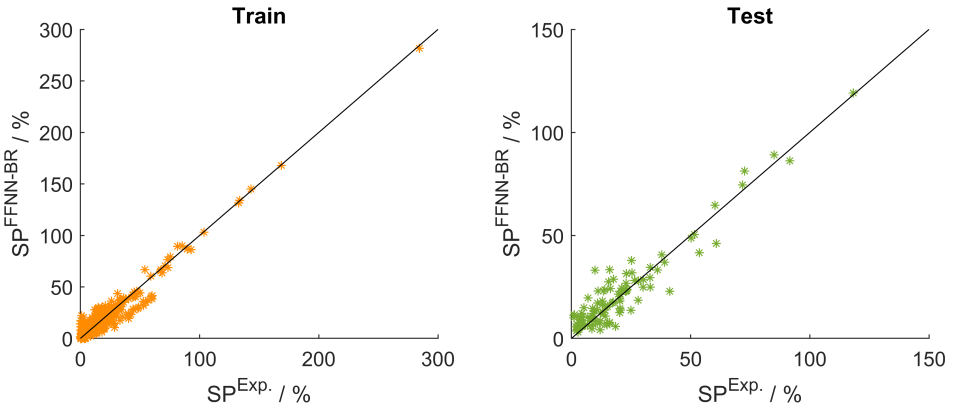

Figure 8: Regression plots of the FFNN-BR model predicted values versus experimental values for SP

the experimental swelling potential. The frequency of the residuals, i.e. difference between experimental and predicted values, of the FFNN-LM follow a normal distribution. The residuals are mostly distributed in the range of -10 to 10 %, indicating an acceptable performance of the model. The modeling residuals for approximately 150 data points equal zero.

Table 8: Statistical indices of various models for predicting clay swelling potential.

Model	Dataset	R^2	MSE	MAE	MAD
FFNN-LM	Train	0.9132	47.51	4.79	16.32
	Test	0.9370	43.85	5.27	15.32
FFNN-BR	Train	0.9322	40.66	4.37	12.57
	Test	0.8870	47.52	5.07	13.30
CFNN-LM	Train	0.9258	43.09	4.60	13.09
	Test	0.8947	58.65	5.47	20.28
CFNN-BR	Train	0.9403	34.08	3.83	12.58
	Test	0.8881	58.52	5.47	13.70

The FFNN-LM model performs the best in determining the swelling potential of soil samples reported by Hakami et al. [63] as the model predictions showed the least deviations from experimental measurements (Table 9). Most of the parameter values in Hakami et al. [63] dataset are in the proximity of mean values in Table 5, which could explain the high efficiency of the FFNN-LM model. For instance, the swelling potential in Hakami et al. [63] is in the range of 18.8 to 34.2 %, which is close to the mean value (SP $=$ 19.79 %) of the compiled dataset. The FFNN-LM showed the lowest predictive quality

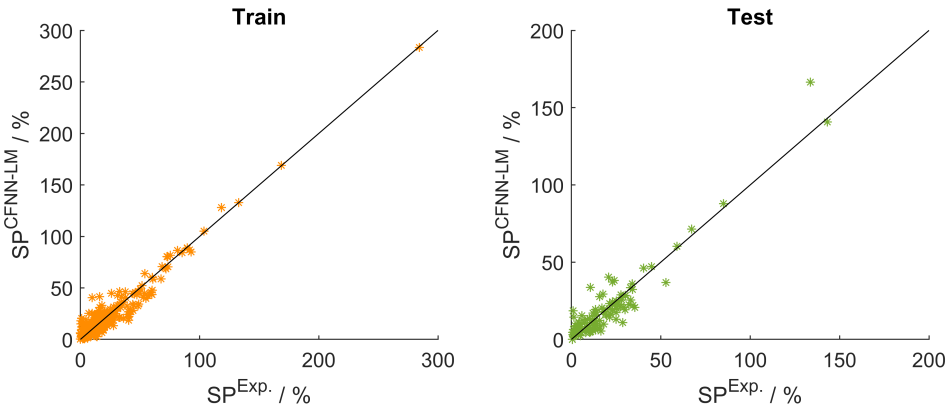

Figure 9: Regression plots of the CFNN-LM model predicted values versus experimental values for SP

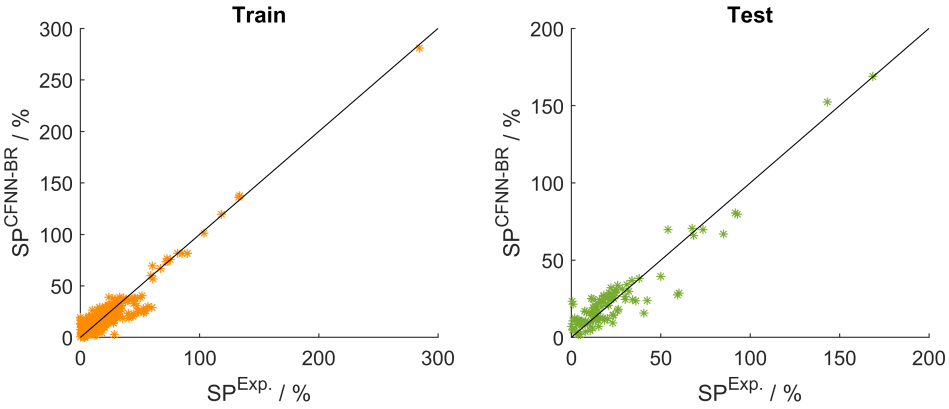

Figure 10: Regression plots of the CFNN-BR model predicted values versus experimental values for SP

in predicting the SP values of Erzin et al. [62] and Snethen et al. [58], especially the experimental values reported by Snethen et al. [58]. The statistical analysis indicates that the model is less accurate in predicting low swelling potentials, i.e. SP values close to 0.01 %, due to the limited experimental data in this range. However, the predictions are sufficiently accurate for practical applications.

Table 9: Evaluating the performance of the FFNN-LM model on various experimental datasets.

Reference	MSE	MAE	MAD
Ashayeri et al. [51]	34.08	5.10	3.46
Çimen et al. [61]	42.24	4.95	6.45
Hakami et al. [63]	13.13	2.85	4.06
Çokça [59]	48.87	5.07	15.88
Surgel [57]	28.39	3.85	9.84
Snethen et al. [58]	180.70	9.53	7.21
Rao et al. [64]	30.57	3.99	8.87
Çokça [60]	56.39	5.32	40.65
Erzin et al. [62]	97.67	7.72	21.11

A William's plot (Figure 12) was sketched on the basis of the calculated standardized residuals and hat values for the FFNN-LM models' outputs. Figure 12 shows that the majority of the data fall within the valid domain, $0 \leq H \leq 0.0077$ and $-3 \leq \text{SR} \leq 3$. The analysis shows that 26 data points corresponding to 5 % of the input dataset are outliers from the applicability domain of the model. The application of the leverage approach showed that the developed model is statistically valid. The invalid points where extremely high or low data points (outliers) observed from the compiled dataset is listed in Table 10.

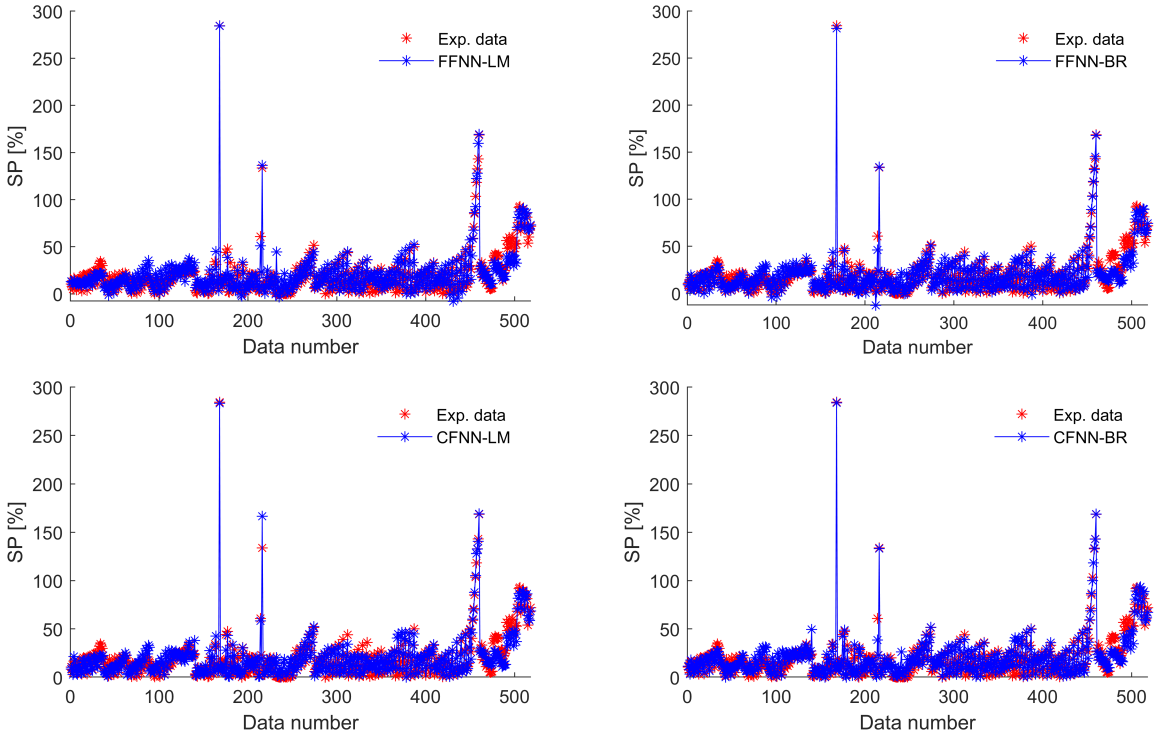

Figure 11: The comparison between the network models and measured values of swelling potential for the input dataset

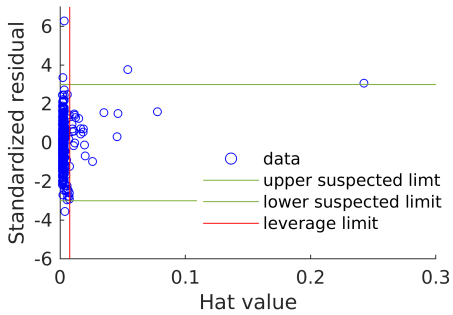

Figure 12: William's plot of clay swelling potential dataset for the FFNN-LM model.

After finalizing the testing, I calculated the parameter impact on the MSE of the FFNN-LM model, testing each of the parameters. The testing proceeded with modifying parameters one at a time to the mean value of the individual parameter values. The parameter impact is displayed in Table 11 in percentage along with the importance ranking of each parameter along with the ranking of relative importance. According to the ranking of parameter impact is as follows: w_{L} and C, I_{P}, A, w_{P}, and w and γ_{d}.

Table 10: Swelling potential outlier for the applicability domain of the FFNN-LM model.

No	A	w (%)	γ_d (kN m^{-3})	w_L (%)	w_P (%)	I_P (%)	C (%)	SP (%)	Ref.
1	1.6	6.4	14.1	146.0	30	116.0	72.5	284.4	Çokça [59]
2	0.8	3.9	12.7	81.0	25	56.0	66.5	44.1	Çokça [59]
3	80.5	10.0	16.4	230.0	28	202.0	2.5	143.2	Çokça [60]
4	90.0	10.0	16.4	255.0	30	225.0	2.5	168.6	Çokça [60]
5	34.8	10.0	16.4	112.0	23	89.0	2.6	71.1	Çokça [60]
6	43.5	10.0	16.4	135.0	24	111.0	2.6	85.0	Çokça [60]
7	50.8	10.0	16.4	155.0	26	129.0	2.5	103.6	Çokça [60]
8	60.9	10.0	16.4	180.0	26	154.0	2.5	118.2	Çokça [60]
9	70.2	10.0	16.4	205.0	28	177.0	2.5	132.7	Çokça [60]
10	1.5	14.6	14.3	108.0	26	82.0	54.8	68.4	Erzin et al. [62]
11	1.5	16.3	15.3	108.0	26	82.0	54.8	75.5	Erzin et al. [62]
12	1.5	16.7	15.9	108.0	26	82.0	54.8	91.6	Erzin et al. [62]
13	1.5	18.7	15.8	108.0	26	82.0	54.8	92.8	Erzin et al. [62]
14	1.5	15.3	14.4	108.0	26	82.0	54.8	67.2	Erzin et al. [62]
15	1.5	15.5	15.2	108.0	26	82.0	54.8	73.3	Erzin et al. [62]
16	1.5	15.7	16.0	108.0	26	82.0	54.8	89.6	Erzin et al. [62]
17	1.5	14.9	16.0	108.0	26	82.0	54.8	89.7	Erzin et al. [62]
18	1.5	20.3	14.7	108.0	26	82.0	54.8	73.5	Erzin et al. [62]
19	1.5	19.5	15.5	108.0	26	82.0	54.8	72.6	Erzin et al. [62]
20	1.5	21.2	16.1	108.0	26	82.0	54.8	85.4	Erzin et al. [62]
21	1.5	19.4	16.1	108.0	26	82.0	54.8	81.4	Erzin et al. [62]
22	1.5	27.7	14.9	108.0	26	82.0	54.8	67.6	Erzin et al. [62]
23	1.5	25.0	15.2	108.0	26	82.0	54.8	71.8	Erzin et al. [62]
24	1.0	20.0	16.0	78.5	25	53.5	56.0	9.9	Rao et al. [64]
25	1.0	39.5	12.8	96.0	38	58.0	57.0	1.0	Snethen et al. [58]
26	1.4	30.0	15.6	128.0	38	89.7	64.0	133.7	Surgel [57]

Table 11: Relative importance of input parameters for swelling potential models

Input parameters	Relative impact of inputs on MSE (%)				Ranking of inputs as per relative importance			
	FFNN-LM	FFNN-BR	CFNN-LM	CFNN-BR	FFNN-LM	FFNN-BR	CFNN-LM	CFNN-BR
A	7	10	4	7	4	4	5	5
w	2	2	4	2	6	6	5	6
γ_d	2	2	3	2	6	6	7	6
w_L	36	26	39	18	1	2	1	3
w_P	4	22	8	9	5	3	4	4
I_P	13	34	19	19	3	1	3	2
C	36	5	23	44	1	5	2	1

4.2 Results - Swelling pressure

4.2.1 Pre-model

Directly after collecting and compiling the swelling pressure data set, I developed a very accurate model. However, after testing the model on each of the smaller datasets with different sources, I realized something is wrong with the dataset from Basma et al. [11] (Table 12).

Table 12: Swelling pressure data set based blah balh

Reference	MSE	MAE	MAD
Rao et al. [64]	333.89	12.42	253.12
Hakami et al. [63]	110.70	6.42	342.63
Basma et al. [11]	11885.04	48.66	737.81
Tonoz et al. [66]	0.95	0.77	446.23
Kayabali et al. [67]	390.25	14.10	423.88

My initial thought on the error cause was that there was a typing error on the specific input. Analyzing the value, I found out that there is only one data input, shown in Table 13, with a completely wrong prediction of the swelling pressure value. Deleting the data input in question changes the overall MSE of the FFNN-LM model from 965.66 to 379.18. However, there was another extreme error that did not share any common properties. Inspecting the research paper published on the data, there was a different problem which is that the researchers used a newly developed testing method to acquire the experimental data.

Table 13: Error data input specification

Data	A	Gravel	Sand	Silt	Clay	w_L	w_P	I_P	γ_d	w	σ^{sw}_{max}	CFNN-LM
Restrained S3	0.76	0	27	39	34	53	27	26	16.5	30	146.70	542.15

4.2.2 Finalized swelling pressure model

The same network models as the ones used for the swelling potential dataset were applied for the swelling pressure dataset. The MSE values of the testing and training phases of each network according to each of the neurons have been traced and depicted in Figure 13. The FFNN-LM model had the most consistent MSE results among the other network structures throughout all 50 neurons. Moreover, the model has an easier visual to perceive the decreasing trend of the error until the number of neurons reaches the lowest point and starts increasing in general. However, not only the low error value was the factor to pick a certain number of neurons as optimal, but also the adjacency of the training and testing error as well as the lesser error value of the test than training. It confirms the generalization ability of the developed model. In this case, the FFNN-LM, the best network model, has 20 neurons in the hidden layer. The FFNN-BR, CFNN-LM, and CFNN-BR networks have 26, 23, and 36 neurons in the hidden layer, respectively.

Regression plots of each swelling pressure prediction models are depicted in Figure 14, Figure 15, Figure 16, and Figure 17 to show accumulation of values around the slope line for experimental values and predicted values for both training and testing datasets. According to statistical analysis, presented in Table 14, all of the models show decent R^2 of over 0.96. In terms of R^2, all of the models give outstanding values, but the MSE also plays a crucial role in the evaluation of these predictive models. There are

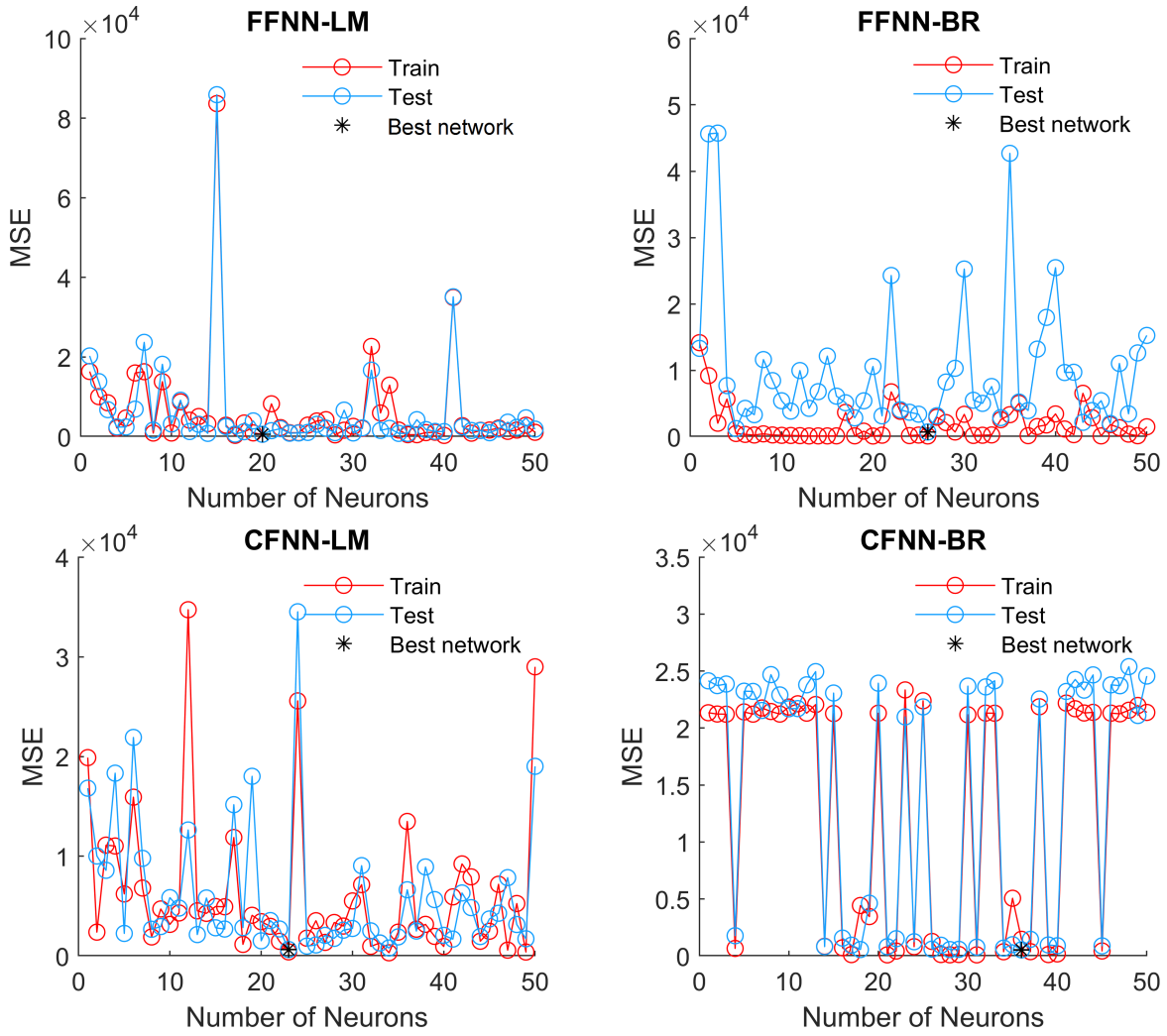

Figure 13: Identifying the optimum number of hidden neurons of all neural network's structures for P_S.

mainly error values in the hundreds which are incomparably high compared to swelling potential prediction models. The reason is that the experimental swelling pressure values are in hundreds to thousands while the swelling potential values are in the early hundreds at most. Thus, comparatively, these MSE values are excellent taking the actual scale of the output parameter. The FFNN-BR has the lowest MSE value on the training dataset, although, the overall predictive ability is more important so that the overall MSE has a higher impact on the ranking of the models. The FFNN-LM has the lowest overall MSE values, making the network the most accurate model. The statistics of the best model indicate R^2, MSE, MAE, and MAD values of 0.9856, 589.2, 17.68, and 293.89, respectively. The developed network models follow the accuracy ranking as FFNN-LM, CFNN-LM, FFNN-BR, and CFNN-BR on the collected dataset.

The accuracy of the predictive models is further depicted in Figure 18 in terms of a response plot. The response plot shows a good agreement between the outputs of the FFNN-LM model and the experimental values. Other models also performed well in predicting the experimental swelling pressure. The frequency of the residuals, i.e. difference between experimental and predicted values, of the FFNN-LM follow a normal distribution. The residuals are mostly distributed in the range of -10 to 10 %, indicating an acceptable performance of the model. The modeling residuals for approximately 200 data points in the given range.

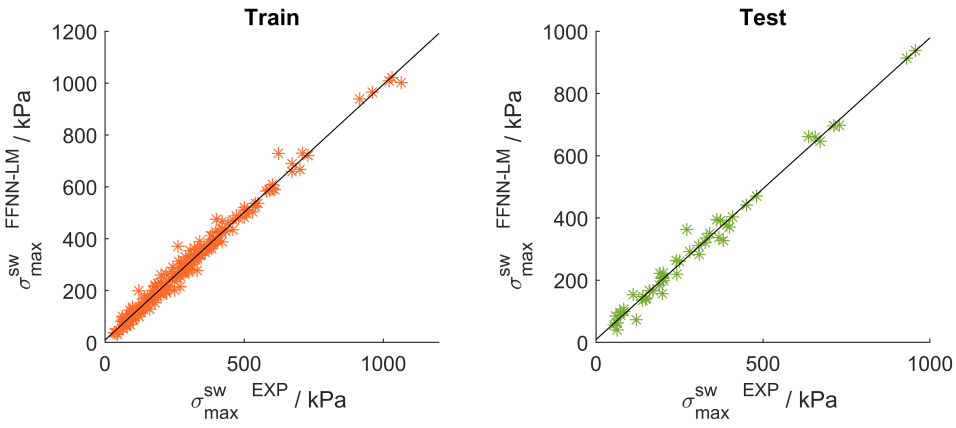

Figure 14: Regression plots of the FFNN-LM model predicted values versus experimental σ^{sw}_{max} values

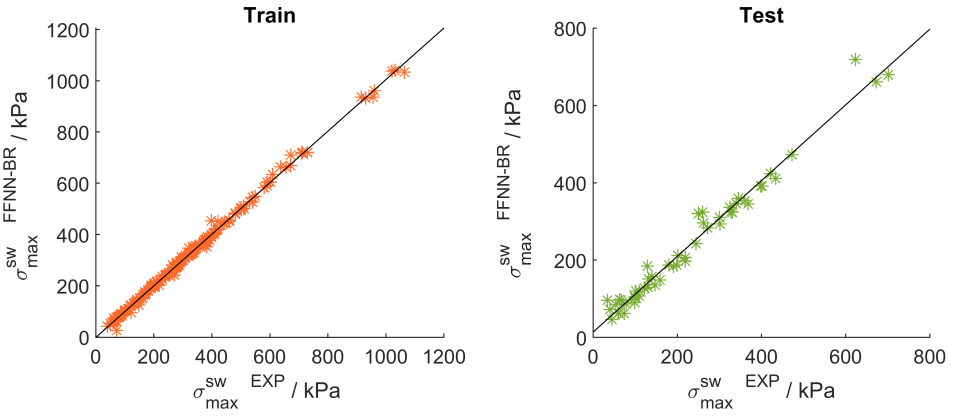

Figure 15: Regression plots of the FFNN-BR model predicted values versus experimental σ^{sw}_{max} values

Model	Dataset	R^2	MSE	MAE	MAD
FFNN-LM	Train	0.9850	587.60	17.51	293.06
	Test	0.9879	595.62	18.35	297.19
FFNN-BR	Train	0.9976	104.01	10.49	304.95
	Test	0.9764	699.88	17.50	239.90
CFNN-LM	Train	0.9908	412.61	13.69	297.85
	Test	0.9833	648.04	18.93	280.64
CFNN-BR	Train	0.9625	1464.46	9.83	283.61
	Test	0.9893	538.16	17.86	294.41

Table 14: Statistical indices of various models for predicting clay swelling pressure.

The FFNN-LM model performs the best in determining the swelling pressure of soil samples reported by Hakami et al. [63] as the model predictions showed the seamlessly perfect performance with the least error (Table 15). Most of the parameter values in Hakami et al. [63] dataset are in the proximity of mean values in Table 6, which could explain the high efficiency of the FFNN-LM model. The FFNN-LM showed the lowest predictive quality in predicting the σ^{sw}_{max} value of Kayabali et al. [67] and Rao et al. [64], especially the experimental values reported by Kayabali et al. [67], which shows a lot higher error.

A William's plot (Figure 12) was sketched based on the calculated standardized residuals and hat values for the CFNN-LM models' outputs. Figure 12 shows that the majority of the data fall within the valid domain, $0 \leq H \leq 0.015$ and $-3 \leq SR \leq 3$. The analysis shows that 21 data points are outliers from the applicability domain of the model. The application of the leverage approach showed that the developed

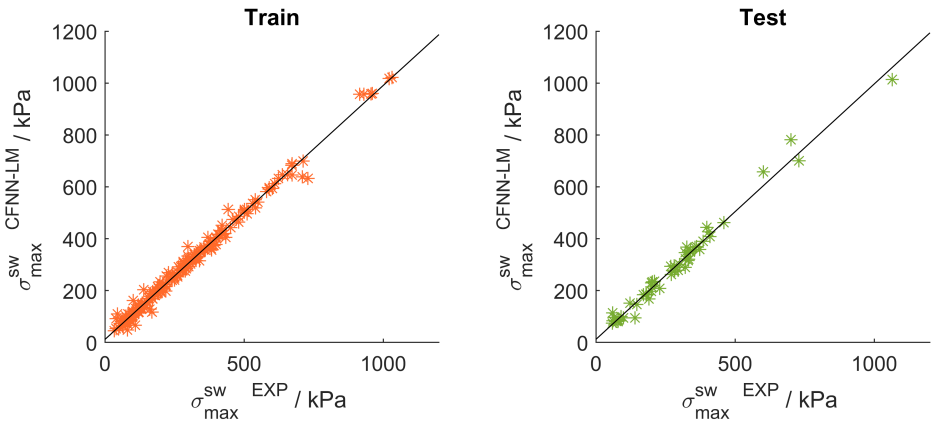

Figure 16: Regression plots of the CFNN-LM model predicted values versus experimental σ^{sw}_{max} values

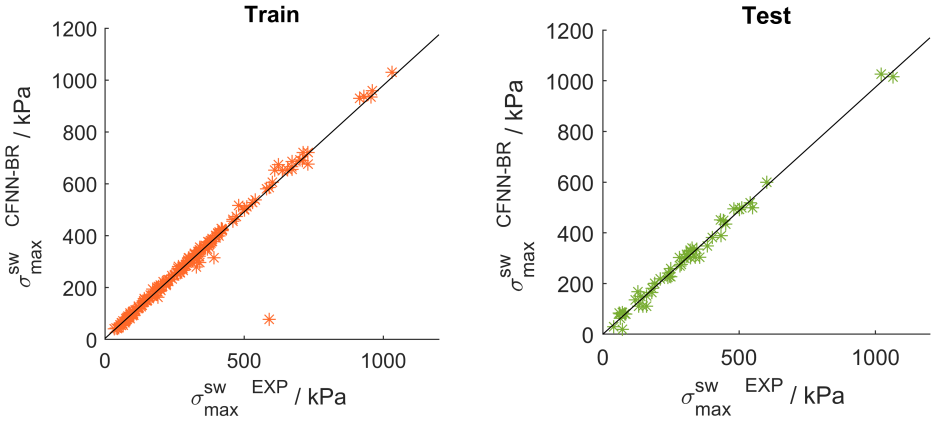

Figure 17: Regression plots of the CFNN-BR model predicted values versus experimental σ^{sw}_{max} values

Table 15: Swelling pressure data set based blah balh

Ref.	MSE	MAE	MAD
Rao et al. [64]	558.16	17.28	121.68
Hakami et al. [63]	335.82	13.50	30.39
Tonoz et al. [66]	346.52	18.16	262.02
Kayabali et al. [67]	1146.61	25.27	315.80

model is statistically valid. The further detailed specification of outliers is shown in Table 16. From the Table 16, it could be noticed that over 70% of the outliers which makes more than 40% of the actual data set size are from Kayabali et al. [67]. The reason lies in the data itself because only Kayabali et al. [67], out of all sources, used customized testing methods while others all used ASTM standards. It could also be derived and concluded that the result from the FFNN-LM model creates swelling pressure results closer to the ASTM standard.

After finalizing the testing, I calculated the parameter impact on the MSE of the FFNN-LM model, testing each of the parameters. The testing proceeded with modifying parameters one at a time to the mean value of the individual parameter values. The parameter impact is displayed in Table 17 in percentage. The relative importance of parameters are ranked as follows: A, w_{L}, γ_{d}, w_{P}, silt, gravel, w, sand, I_{P}, and C.

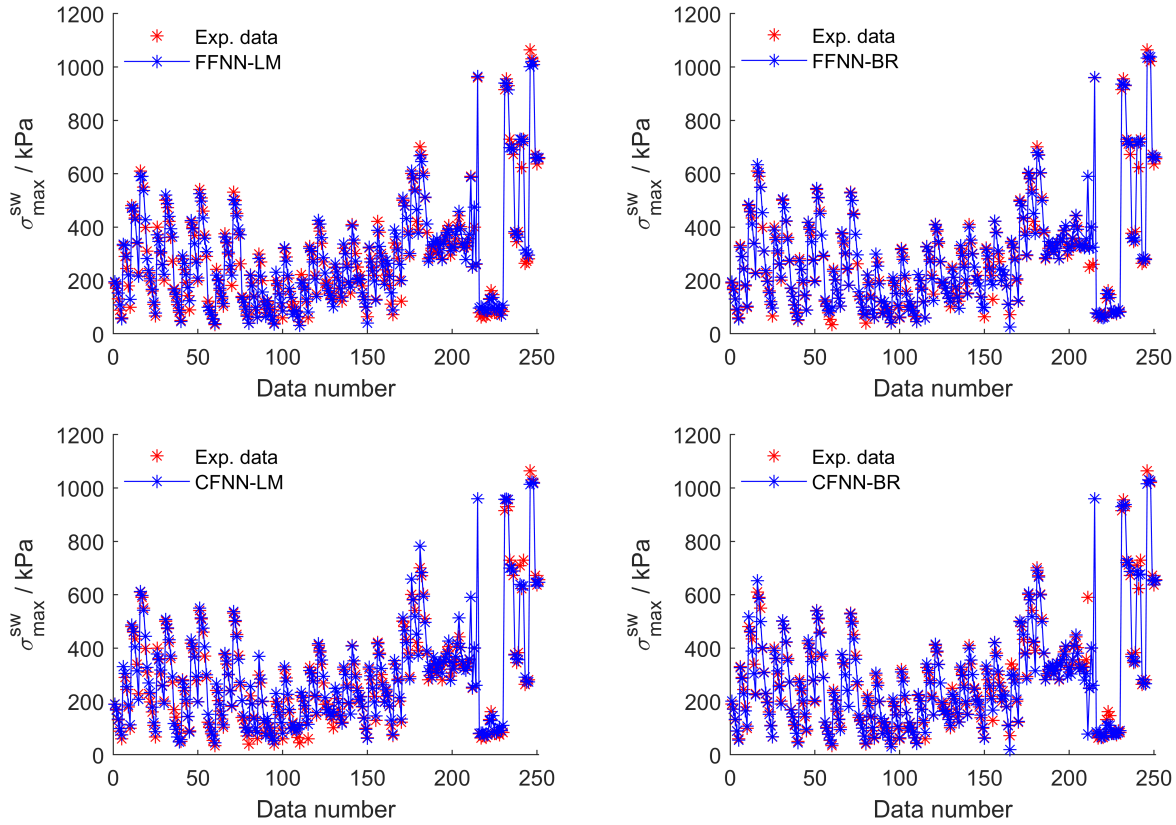

Figure 18: The comparison between the network models and measured values of swelling potential for the input dataset

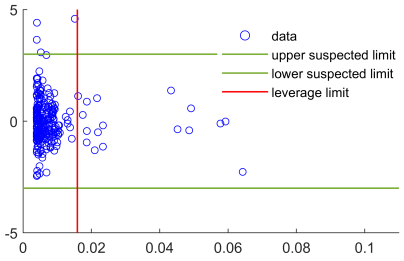

Figure 19: William's plot of clay swelling pressure dataset for the FFNN-LM model.

Table 16: Swelling pressure outlier for the applicability domain of the FFNN-LM model.

No.	A	Gravel (%)	Sand (%)	Silt (%)	C (%)	w_{L} (%)	w_{P} (%)	I_{P} (%)	γ_d (kN/m^3)	w (%)	σ_{max}^{sw} (kPa)	Ref.
1	1.47	0.00	7.00	42.00	51.00	93.00	18.00	75.00	18.00	20.00	272.40	Rao et al. [64]
2	0.88	0.00	1.00	39.50	59.50	74.50	22.00	52.50	18.00	20.00	262.05	Rao et al. [64]
3	3.64	0.00	16.00	48.00	36.00	148.00	17.00	131.00	18.00	0.00	700.88	Rao et al. [64]
4	3.64	0.00	16.00	48.00	36.00	148.00	17.00	131.00	18.00	5.00	671.30	Rao et al. [64]
5	0.56	9.00	15.00	24.00	52.00	66.00	37.00	29.00	14.91	30.00	400.00	Tonoz et al. [66] 2003
6	0.79	10.50	13.10	33.40	43.00	68.00	34.00	34.00	13.64	33.00	960.00	Tonoz et al. [66] 2003
7	0.91	0.00	5.00	40.00	55.00	83.00	33.00	50.00	19.62	25.80	915.00	Kayabali et al. [67]
8	0.91	0.00	5.00	40.00	55.00	83.00	33.00	50.00	19.62	25.60	956.00	Kayabali et al. [67]
9	0.91	0.00	5.00	40.00	55.00	83.00	33.00	50.00	19.42	24.90	930.00	Kayabali et al. [67]
10	0.77	0.00	2.00	28.00	70.00	84.00	30.00	54.00	19.91	25.30	729.00	Kayabali et al. [67]
11	0.77	0.00	2.00	28.00	70.00	84.00	30.00	54.00	19.91	25.20	712.00	Kayabali et al. [67]
12	0.77	0.00	2.00	28.00	70.00	84.00	30.00	54.00	19.72	26.20	672.00	Kayabali et al. [67]
13	0.93	0.00	8.00	46.00	46.00	74.00	31.00	43.00	19.91	24.30	709.00	Kayabali et al. [67]
14	0.93	0.00	8.00	46.00	46.00	74.00	31.00	43.00	19.91	25.00	623.00	Kayabali et al. [67]
15	0.93	0.00	8.00	46.00	46.00	74.00	31.00	43.00	19.82	24.80	729.00	Kayabali et al. [67]
16	1.03	0.00	3.00	38.00	59.00	93.00	32.00	61.00	19.62	24.40	1064.00	Kayabali et al. [67]
17	1.03	0.00	3.00	38.00	59.00	93.00	32.00	61.00	19.82	24.50	1031.00	Kayabali et al. [67]
18	1.03	0.00	3.00	38.00	59.00	93.00	32.00	61.00	19.72	24.30	1021.00	Kayabali et al. [67]
19	0.86	0.00	7.00	36.00	57.00	79.00	30.00	49.00	19.62	25.30	672.00	Kayabali et al. [67]
20	0.86	0.00	7.00	36.00	57.00	79.00	30.00	49.00	19.62	25.70	637.00	Kayabali et al. [67]
21	0.86	0.00	7.00	36.00	57.00	79.00	30.00	49.00	19.62	25.50	656.00	Kayabali et al. [67]

Table 17: Relative importance of input parameters for swelling pressure models

Input parameters	Relative impact of inputs on MSE (%)				Ranking of inputs as per relative importance			
	FFNN-LM	FFNN-BR	CFNN-LM	CFNN-BR	FFNN-LM	FFNN-BR	CFNN-LM	CFNN-BR
A	21	34	2	17	1	1	8	1
Gravel	7	2	1	4	6	10	10	10
Sand	5	7	7	8	8	5	5	7
Silt	8	3	21	9	5	8	2	5
C	3	4	35	13	10	7	1	4
w_{L}	17	7	9	5	2	5	4	9
w_{P}	13	14	5	16	4	3	6	2
I_{P}	4	16	16	9	9	2	3	5
γ_{d}	15	9	3	14	3	4	7	3
w	7	3	1	6	6	8	9	8

4.3 Comparative analysis on swelling potential

We used the experimental clay swelling potential data from the dataset to further scrutinize the performance of the model. Furthermore, the predictive ability of the FFNN-LM model was further compared with Basma [27], Nayak et al. [25], and Seed et al. [26] correlations. The designed comparison analysis provides an in-depth understanding of the physical behavior of the model, and its overall performance to determine the swelling potential of clayey soils in a wide range of conditions.

The initial water content and soil dry unit weight affect the stress state and structure of compacted soils, which in turn influence the swelling properties. Çimen et al. [61] collected four different disturbed clay samples with high plasticity from four regions in Turkey that have different water content and dry unit weight. The comparison analysis, depicted in Figure 20, shows that for any constant dry unit weight, soil swelling potential decreases with increasing the initial water content. Furthermore, at a constant water content, the swelling potential increases with increasing the dry unit weight. The deviations at most points are minor, confirming the acceptable performance of the model in predicting the experimental values. The predictions of the FFNN-LM model are less accurate where the water content equals 15 and 20 % because the training data points with these water contents rare.

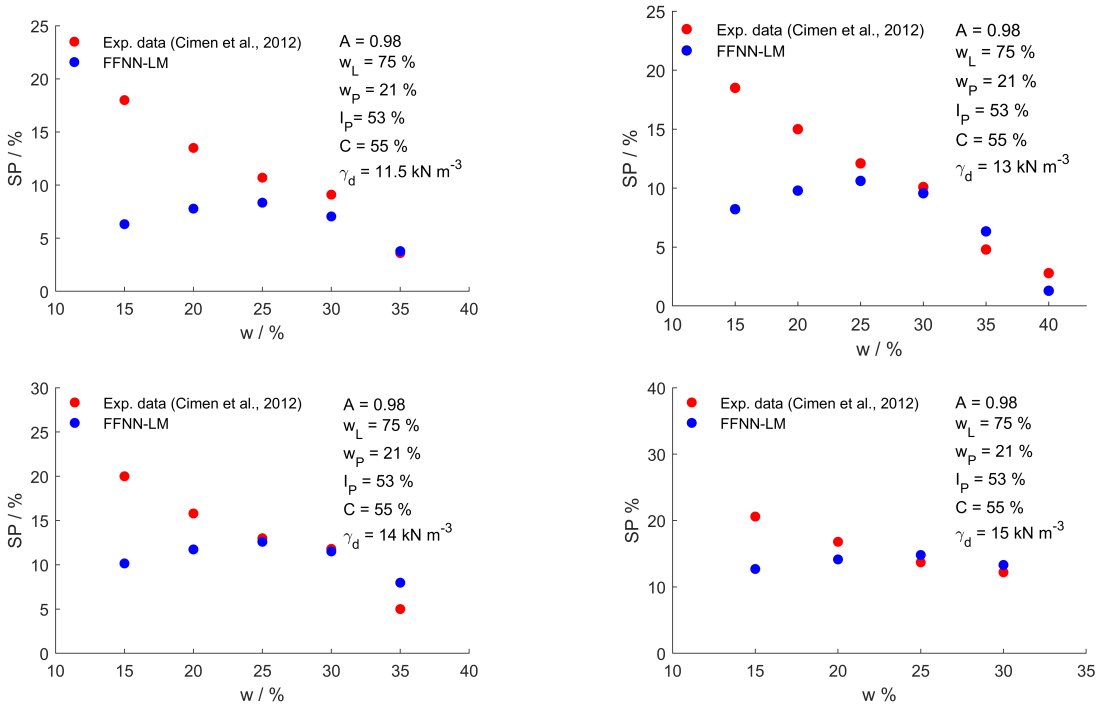

Figure 20: Swelling potential of clay soils with high plasticity and varying moisture contents and dry unit weights reported by Çimen et al. [61] and estimated by the FFNN-LM model.

Rao et al. [64] provided experimental data of 10 remolded expansive soil samples collected from 10 districts of the state of Andhra Pradesh in India. The clay content of the dataset varies between 36 and 88 %, while the plasticity index changes between 36 and 131 %. The analysis shows that the model can accurately predict the experimental swelling potential reported by Rao et al. [64]. Furthermore, the model can capture the trend observed in the experimental data (Figure 21 and Figure 22), i.e. the increase of swelling potential with increasing dry unit weight. It is evident that the model is able to determine the swelling potential at wide ranges of soil plasticity.

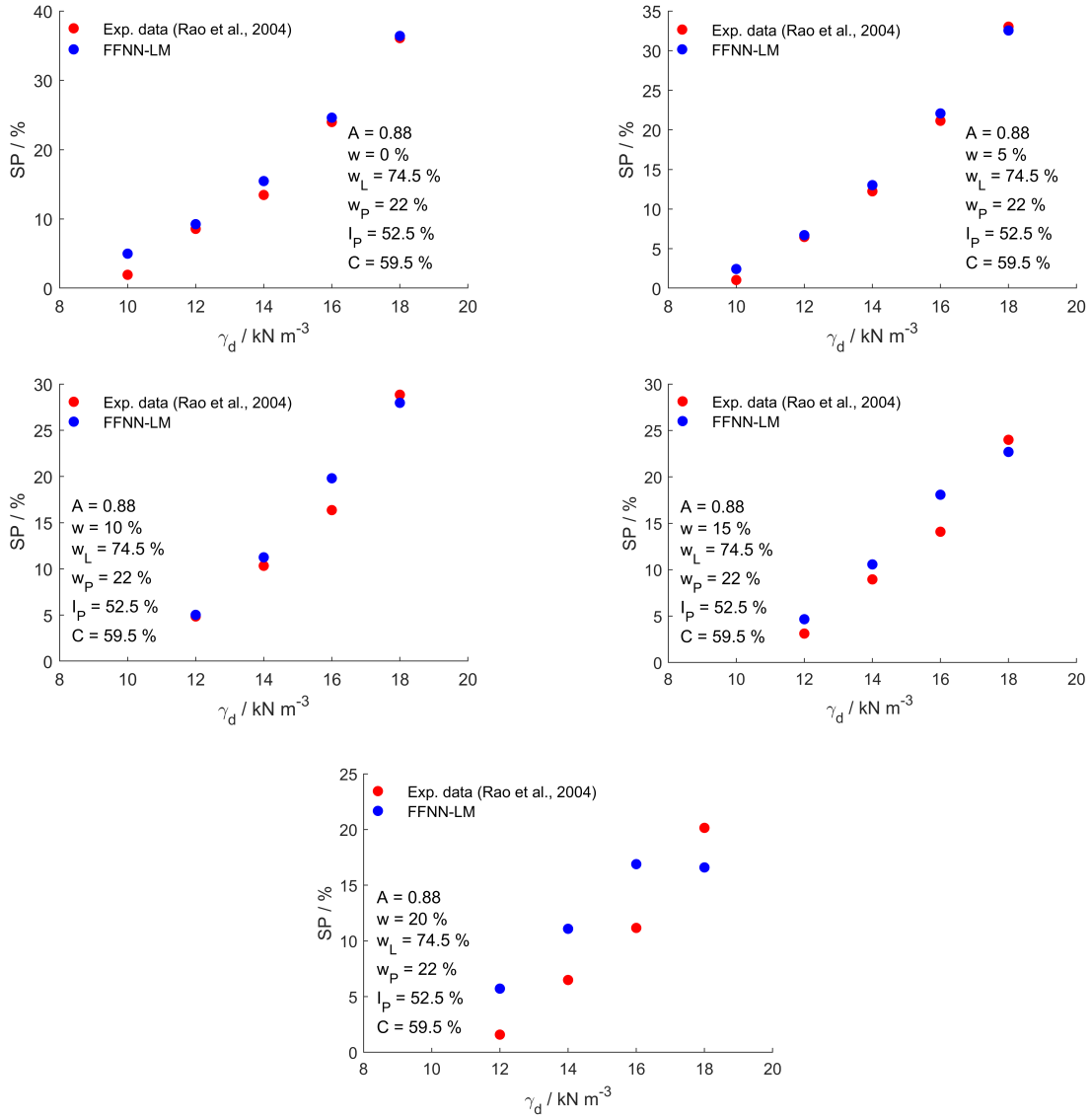

Figure 21: Swelling potential of remolded expansive soil with plasticity index of 52.5% and varying moisture contents and dry unit weights reported by Rao et al. [64] and estimated by the FFNN-LM model.

Figure 23 compares the experimental and predicted swelling potential with varying values of dry unit weight, activity, liquid limit, and plasticity index. The model can determine the swelling potential of expansive soils over a wide range of conditions. For instance, the plasticity index of the soil samples reported by Çokça [60] varies between 28 and 225 %. The model predicted values are in good agreement with the experimental ones.

The predictive ability of the FFNN-LM model was compared with three empirical and semi-empirical correlations, i.e., Basma [27], Nayak et al. [25], and Seed et al. [26]. To ensure the fairness of the comparison, only the data points falling within the applicability domain of each correlation were considered. For example, we only used 68 data points to analyze the predictive performance of Nayak et al. [25] (Equation 7) as limited data points fall within the applicability domain of this correlation. The statistical indices presented in Table 18 indicate that the FFNN-LM outperforms all correlations in predicting the clay swelling potential over the range of conditions reported in this study. The analysis shows that all the employed correlations fail in determining the swelling potential.

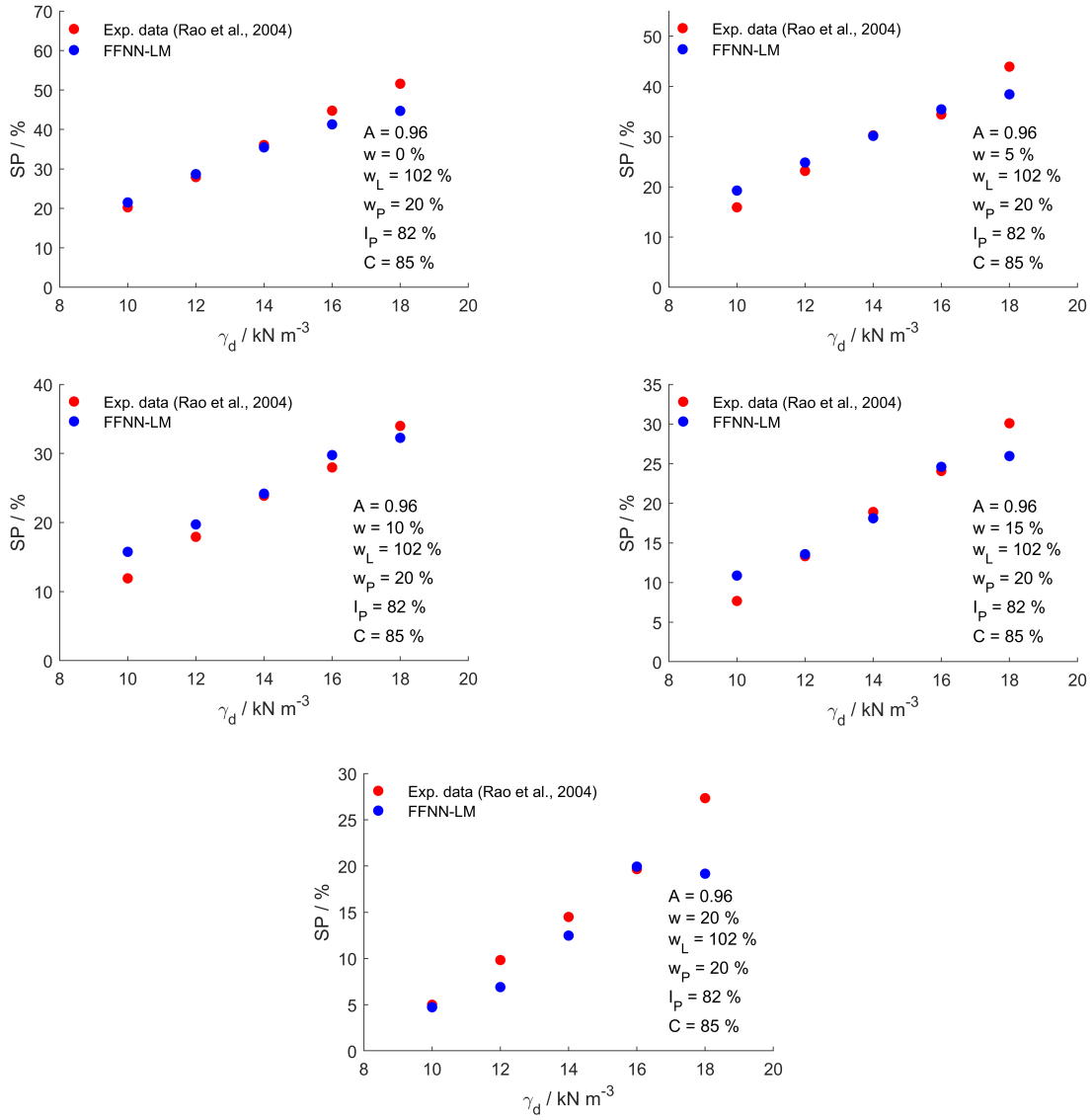

Figure 22: Swelling potential of remolded expansive soil with a plasticity index of 82% and varying water contents and dry unit weights reported by Rao et al. [64] and estimated by the FFNN-LM model.

Table 18: Performance evaluation of predictive models.

Prediction method	R^2	MSE	MAE	MAD
FFNN-LM (518 data points)	0.919	46.75	4.88	12.74
Basma [27] (450 data points)	0.067	1925.20	26.73	26.53
Nayak et al. [25] (Equation 7) (68 data points)	0.288	1488.34	27.05	34.44
Nayak et al. [25] (Equation 8) (473 data points)	0.021	5074.38	38.22	39.96
Seed et al. [26] (Equation 9) (68 data points)	0.319	1368.20	26.62	28.11
Seed et al. [26] (Equation 10) (518 data points)	0.297	18972.11	31.94	66.14

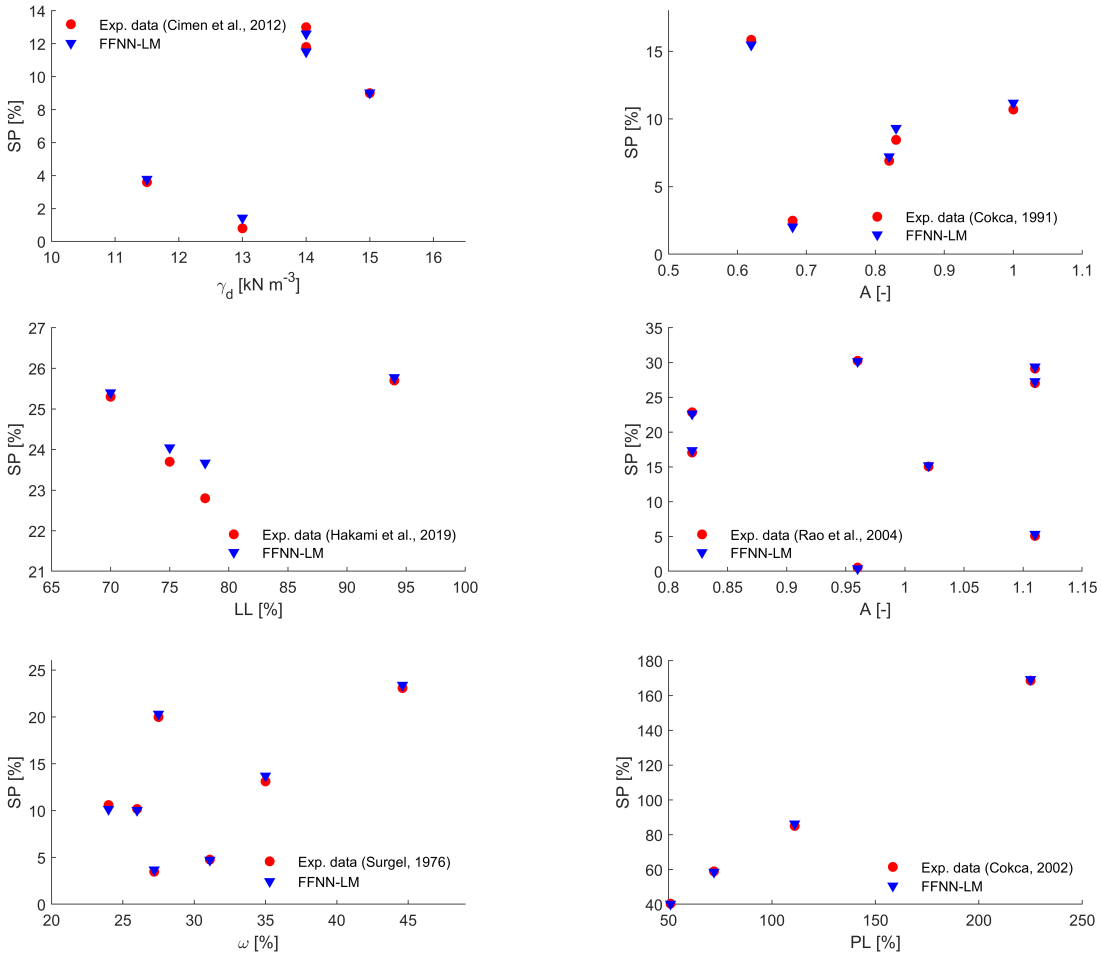

Figure 23: Swelling potential of various expansive soils reported by Çimen et al. [61], Çokça [59], Çokça [60], Hakami et al. [63], Rao et al. [64], and Surgel [57] and estimated by the FFNN-LM model.

4.4 Comparative analysis on swelling pressure

We further inspected the swelling pressure data from the experimental clay dataset to acknowledge the performance of the model. Moreover, the predictive ability of the FFNN-LM model was further compared with Abiddin Erguler et al. [85], Wu et al. [87], Nayak et al. [25] and Cantillo et al. [86] correlations. The designed comparison analysis provides an in-depth understanding of the physical behavior of the model, and its overall performance to determine the swelling pressure of clayey soils in a wide range of conditions.

The comparative analysis of the FFNN-LM model for swelling pressure was specifically done on the dataset from Rao et al. [64] as experimental testing was more systematic. In Figure 24,Figure 25, Figure 26, and Figure 27, I tried to show the FFNN-LM prediction performance at different moisture content and dry unit weight as well as the relationship between the parameters and the swelling pressure. Rao et al. [64] collected ten different remolded and compacted clay samples with highly varying parametric values except for gravel content. The clay content of the dataset Rao et al. [64] varies between 36 and 85 %, while the plasticity index changes between 36 and 131 %. The collected samples were tested under controlled moisture content, and initial dry unit weights to determine swelling pressure dependency on these parameters.

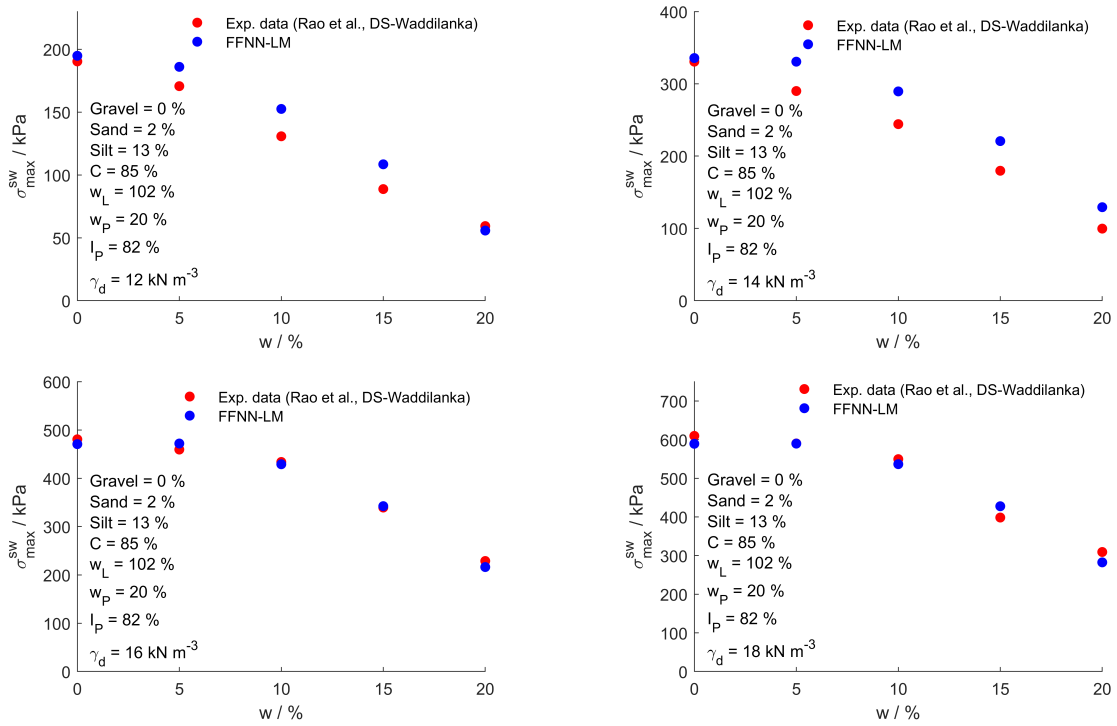

Figure 24: Swelling pressure of clay soils with high plasticity and varying moisture contents and dry unit weights reported by Wadillanka from Rao et al. [64] and estimated by the FFNN-LM model.

The comparison analysis, depicted in Figure 24 ,Figure 26, shows that for any constant dry unit weight, the swelling pressure of soil decreases with increasing the initial water content. Also, Figure 25,Figure 27 demonstrates the swelling pressure increase with increasing the dry unit weight at a constant water content. Furthermore, Figure 24, and Figure 25 and Figure 26, and Figure 27 are demonstrated on exact same dataset individually for further analysis. The deviations at most points are minor, confirming the acceptable performance of the model in predicting the experimental values.

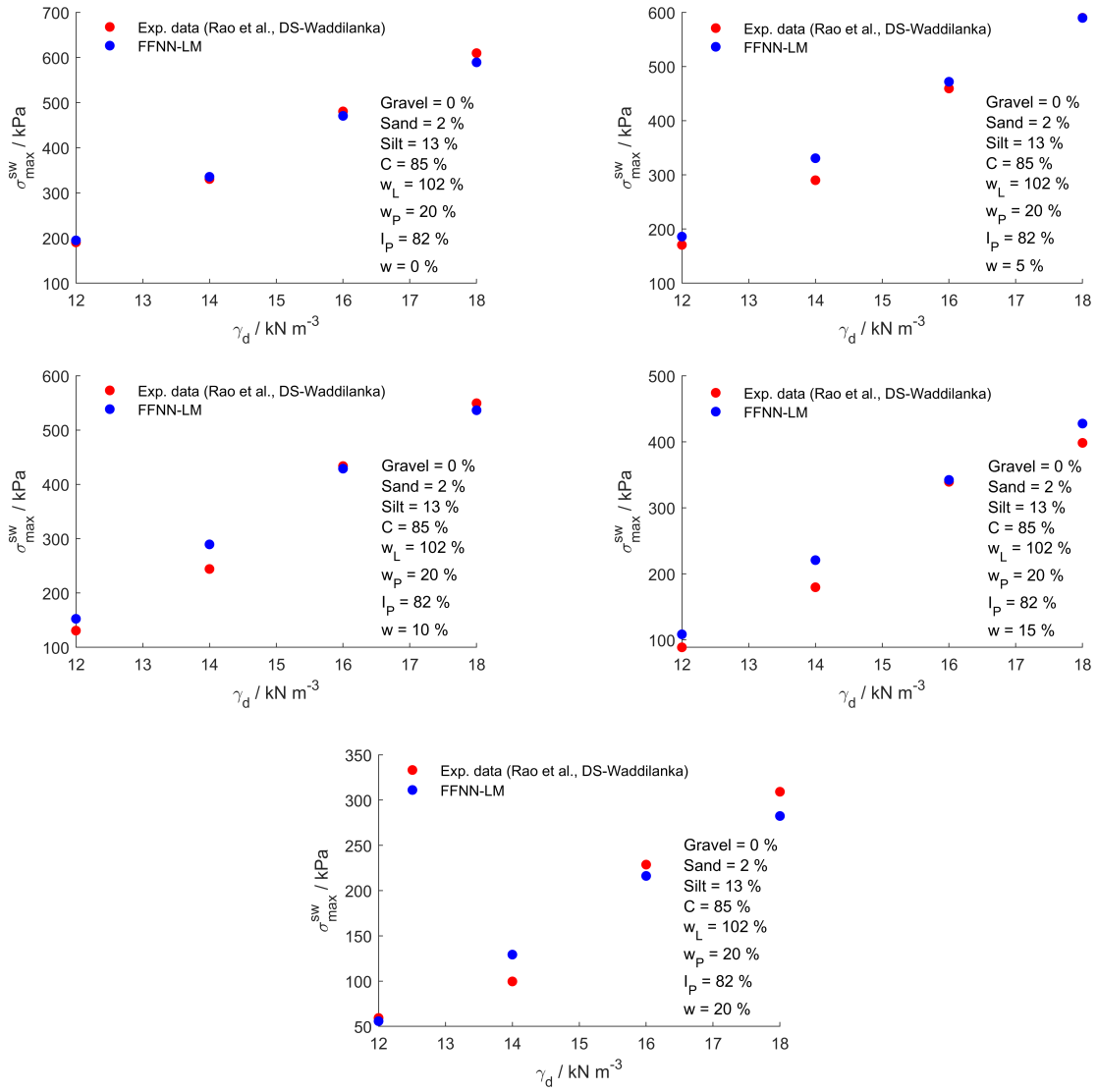

Figure 25: Swelling pressure of clay soils with high plasticity and varying moisture contents and dry unit weights reported by Wadillanka from Rao et al. [64] and estimated by the FFNN-LM model.

Prediction models	R^2	MSE	MAE	MAD
FFNN-LM	0.9865	589.22	17.68	148.24
Abiddin Erguler et al. [85] (251 data points)	0.2033	208444.99	357.70	320.88
Cantillo et al. [86] (Equation 12) (214 data points)	0.0024	127890.48	283.35	177.96
Cantillo et al. [86] (Equation 13) (251 data points)	0.0052	1273677.30	781.60	716.31
Nayak et al. [25] (214 data points)	0.0006	141484.52	271.19	102.54
Wu et al. [87] (Equation 14) (251 data points)	0.008	162646.84	326.83	183.26
Wu et al. [87] (Equation 15) (214 data points)	0.001	155151.38	309.30	0.01

The predictive ability of the FFNN-LM model was compared with three empirical and semi-empirical correlations, i.e., Wu et al. [87], Nayak et al. [25], Cantillo et al. [86] and Abiddin Erguler et al. [85]. To ensure the fairness of the comparison, only the data points falling within the applicability domain of each correlation were considered. For example, we only used 214 data points to analyze the predictive performance of Nayak et al. [25] as limited data points fall within the applicability domain of this correlation. The statistical indices presented in Table 18 indicate that the FFNN-LM outperforms all correlations in predicting the clay swelling potential over the range of conditions reported in this study. The analysis

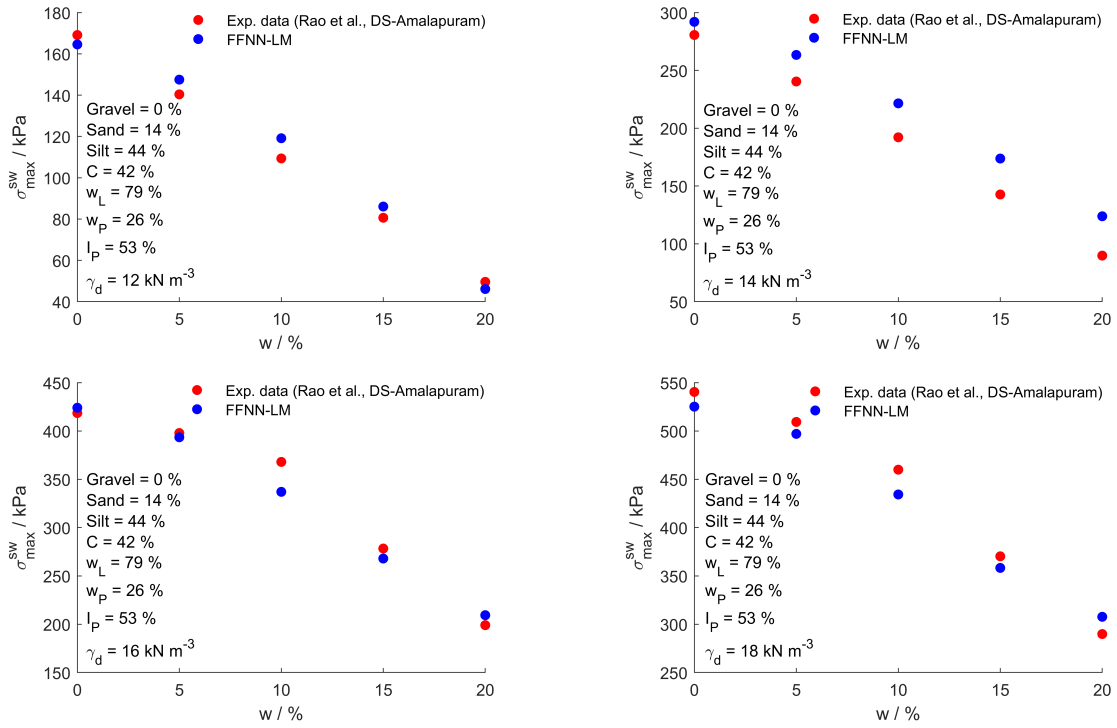

Figure 26: Swelling pressure of clay soils with high plasticity and varying moisture contents and dry unit weights reported by Amalapuram from Rao et al. [64] and estimated by the FFNN-LM model.

shows that all the employed correlations fail in determining the swelling pressure.

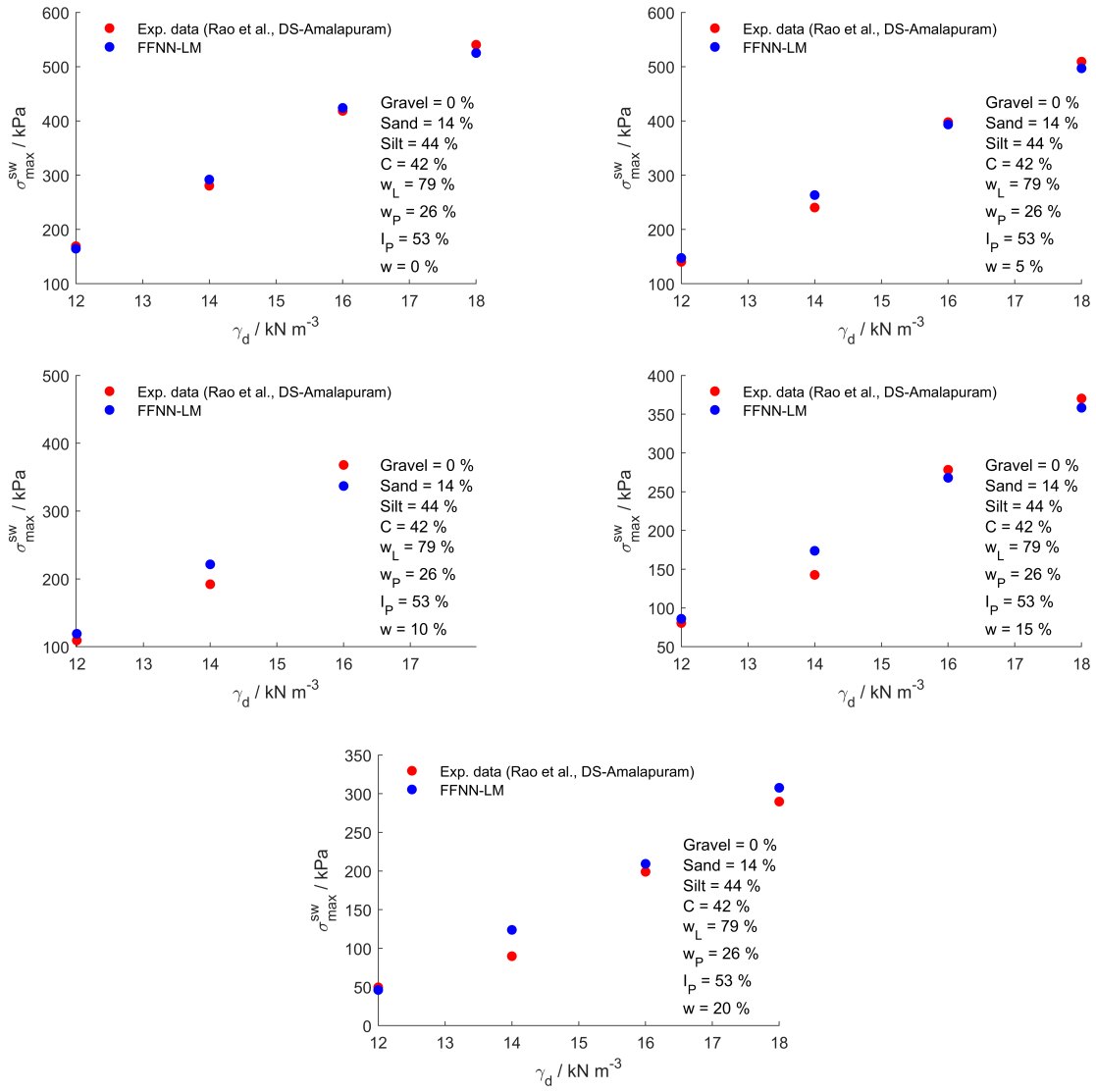

Figure 27: Swelling pressure of clay soils with high plasticity and varying moisture contents and dry unit weights reported by Amalapuram from Rao et al. [64] and estimated by the FFNN-LM model.

5 Discussion

Concluding the presented results, the FFNN-LM model estimates with sufficient accuracy on expansive soil with several clay types and at a practical range of swelling potential, employing simple parameters to measure. Compared to existing empirical correlations and ANN models, FFNN-LM used a larger dataset at a more extensive scale. Generally, the model provides accurate results except for soil with negligible swelling potential. Hence, the model is convenient for geological applications.

The FFNN-LM model developed for swelling pressure estimation provides accurate results on various types of natural clay per ASTM standards. Based on the sheer size of the dataset and parameters, the model has the most extensive scale among the reviewed AI models. Also, the performance analysis of the FFNN-LM model shows superior results compared to existing empirical correlations and ANN models. Overall, the model predicts within an acceptable range of errors for the dataset range given in Table 6.

Further application of the FFNN-LM model should be under the same dataset circumstances as the modeler used to build it. If the model is applied for predicting outside its range, the modeler should decide whether the deviation is in an acceptable spectrum. Future studies may build similar models splitting and enlarging the dataset into several groups by its range to increase accuracy for its domain. Even though the training dataset improves with its size, building an organized dataset could prove to be superior. For example, test the same clay repetitively at different conditioning such as increasing moisture content, clay content, or moisture content. As a result, the model could comprehend unknown factors that are affecting the swelling potential, which scientists were not able to identify. Besides, other data-driven models on the existing dataset could improve the FFNN-LM model.

We follow from the presented results that the FFNN-LM model is able to determine the swelling potential of several clay types in a practical range of applications. The model depends on several influential parameters, measured commonly in laboratory testing. Compared to the existing empirical and semi-empirical correlations as well as the AI models, FFNN-LM employs a larger dataset at a more extensive scale. Generally, the model provides accurate results except for soils with negligible swelling potential. The model presented here can be seen as a precise alternative to determine the swelling potential of clayey soils needed for geotechnical projects such as tunneling and bridge construction.

Further application of the FFNN-LM model should be under the range of conditions for which the model was trained. Indeed the model can be applied to determine the clay swelling potential outside of this specified domain, even though it is subjected to the modeler's judgment to decide whether the prediction deviations are in an acceptable spectrum. An accurate and sufficiently large dataset plays a critical role in the development of neural network models. Although we used an adequately large dataset to develop the model, future studies may enlarge the dataset to improve the accuracy and generalization ability of the model. Besides, other optimization algorithms, such as metaheuristics algorithms, can be tested to improve the performance of the network models.

6 Conclusions and Outlook

6.1 Conclusions

This thesis study employed feed-forward and cascade-forward neural networks trained with Levenberg-Marquardt and Bayesian regularization algorithms to determine the swelling potential and swelling pressure of clayey soil. An experimental dataset collected from the literature was used to develop the network models. The predicted swelling potential and swelling pressure were compared with experimental data as well as empirical and semi-empirical correlations. The following main conclusions can be drawn for both of the swelling potential and swelling pressure:

- All four NN models provide satisfactory performance for predicting the swelling potential of clayey soils.
- The FFNN-LM is identified as the most accurate model for the swelling potential regression task, having R^2 and MSE values equal to 0.919 and 46.75, respectively.
- The application of the Leverage method confirmed the accuracy and statistical validity of the swelling potential model, and 5 % of the data were outliers from the applicability domain of the model.
- For each of the models, parameters had a different amount of impact, but a general trend is observed. The top 3 important parameters for swelling potential ANN models are: w_{L}, I_{P}, and C.
- The FFNN-LM is identified as the most accurate model for the swelling pressure regression task, having R^2 and MSE values equal to 0.9865 and 589.22, respectively.
- The application of the Leverage method confirmed the accuracy and statistical validity of the swelling pressure model, and 8 % of the data were outliers from the applicability domain of the model.
- The overall top 3 important parameters for swelling pressure estimation ANN models are: A, w_{L}, and γ_{d}.
- The FFNN-LM model outperforms the examined empirical and semi-empirical correlations, having higher prediction accuracy. This demonstrates the potential of the model to be used as an alternative tool to the otherwise typically employed correlations for determining the clay swelling potential.
- The developed model is reliable and suitable for application in geotechnical projects. One of the key advantages of the model is its ability to cover a broad range of conditions for which the model was trained.

6.2 Outlook

This thesis study is immature in several factors, mostly in the data extraction part. Further research in this soil behavior related model development for expansive soil could take these into consideration:

- The dataset used for the study is not comprehensive enough in terms of the number of parameters as well as parametric values. Chemical parameters are not included in the model development, along with seemingly influential physical parameters such as temperature, soil suction, cation exchange capacity, etc. The input data values have the potential to be aligned systematically by doing tests to cover a wide range of values evenly.

- The working mechanism of ANN models is relatively complicated, where the exclusion of parameters could increase the accuracy of the model. This study did not attempt models with different parameter combinations as the given time frame was not enough. Hence, further model development on the existing data is available for more promising possibilities.

- Artificial/man-made soil samples are not included in swelling pressure model. These expansive soils such as pure bentonite and kaolinite have higher swelling properties. Thus, the model get higher applicability range.

- Future research could focus on other intelligence models such as SVM and convolutional neural network models to evaluate the behavior of swelling properties.

References

[1] Jones Lee. "Shrinking and swelling soils in the UK; assessing clays for the planning process". In: *Earthwise (Keyworth)* Keyworth (2002), pp. 22–23.

[2] John Nelson et al. *Expansive soils: problems and practice in foundation and pavement engineering*. John Wiley & Sons, 1997.

[3] Masoumeh Mokhtari et al. "Swell-shrink behavior of expansive soils, damage and control". In: *Electronic Journal of Geotechnical Engineering* 17 (2012), pp. 2673–2682.

[4] A. S. Bains et al. "Molecular Modelling of The Mechanism of Action of Organic Clay-Swelling Inhibitors". In: *Molecular Simulation* 26.2 (2001), pp. 101–145. DOI: 10.1080/08927020108023012.

[5] Rogers Evarist Swai. "A review of molecular dynamics simulations in the designing of effective shale inhibitors: application for drilling with water-based drilling fluids". In: *Journal of Petroleum Exploration and Production Technology* 10.8 (Dec. 2020), pp. 3515–3532.

[6] Artur Meleshyn et al. "The gap between crystalline and osmotic swelling of Na-montmorillonite: A Monte Carlo study". In: *The Journal of Chemical Physics* 122.3 (2005). DOI: 10.1063/1.1834499.

[7] J. Mering. "On the hydration of montmorillonite". In: *Trans. Faraday Soc.* 42 (1946), pp. 205–219. DOI: 10.1039/TF946420B205.

[8] Richard. W. Mooney et al. "Adsorption of Water Vapor by montmorillonite. II. Effect of exchangeable ions and lattice swelling as measured by X-ray diffraction". In: *Journal of the American Chemical Society* 74.6 (Mar. 1952), pp. 1371–1374. DOI: 10.1021/ja01126a002.

[9] Richard. L. Anderson et al. "Clay swelling - A challenge in the oilfield". In: *Earth-Science Reviews* 98.3 (2010), pp. 201–216. DOI: 10.1016/j.earscirev.2009.11.003.

[10] Faruk Civan. "CHAPTER 2 - MINERALOGY AND MINERAL SENSITIVITY OF PETROLEUM-BEARING FORMATIONS11Parts of this chapter have been reprinted with permission of the Society of Petroleum Engineers from Civan (1999a and 2001c)." In: *Reservoir Formation Damage (Second Edition)*. Ed. by Faruk Civan. Second Edition. Burlington: Gulf Professional Publishing, 2007, pp. 13–77. ISBN: 978-0-7506-7738-7. DOI: https://doi.org/10.1016/B978-075067738-7/50003-8.

[11] Adnan A. Basma et al. "Laboratory assessment of swelling pressure of expansive soils". In: *Applied Clay Science* 9.5 (1995), pp. 355–368. DOI: 10.1016/0169-1317(94)00032-L.

[12] D. E. McCormack et al. "Soil Properties influencing swelling in Canfield and Geeburg Soils". In: *Soil Science Society of America Journal* 39.3 (1975), pp. 496–502. DOI: https://doi.org/10.2136/sssaj1975.03615995003900030034x.

[13] Colin William Gray et al. "Relationships between shrinkage indices and soil properties in some New Zealand soils". In: *Geoderma* 108.3 (2002), pp. 287–299. DOI: https://doi.org/10.1016/S0016-7061(02)00136-2.

[14] El Sohby MA; Rabba EA. "Some factors affecting swelling of clayey soils". In: *GEOTECH. ENG.; ISSN 0046-5828; THA; DA. 1981; VOL. 12; NO 1; PP. 19-39; BIBL. 1 P.; 2 TAB. ; ILL./TABL.* (1981).

[15] J. C. Parker et al. “An evaluation of several methods of estimating soil volume change”. In: *Soil Science Society of America Journal* 41.6 (1977), pp. 1059–1064. DOI: https://doi.org/10.2136/sssaj1977.03615995004100060008x.

[16] Robert D Holtz et al. *An introduction to geotechnical engineering*. Vol. 733. Prentice-Hall Englewood Cliffs, 1981.

[17] Lee Jones et al. “Expansive Soils”. In: Jan. 2012, pp. 413–441. ISBN: 978-0-7277-5707-4. DOI: 10.1007/978-3-319-12127-7_118-1.

[18] Magdi ME Zumrawi et al. “Damages of buildings on expansive soils: diagnosis and avoidance”. In: *International Journal of Multidisciplinary and Scientific Emerging Research* 6.2 (2017), pp. 108–115.

[19] Magdi ME Zumrawi. “Construction problems of light structures founded on expansive soils in Sudan”. In: (2015).

[20] Erich Pimentel. “Existing Methods for Swelling Tests – A Critical Review”. In: *Energy Procedia* 76 (2015). European Geosciences Union General Assembly 2015 - Division Energy, Resources and Environment, EGU 2015, pp. 96–105. ISSN: 1876-6102. DOI: https://doi.org/10.1016/j.egypro.2015.07.857.

[21] Erich Pimentel. “Existing methods for swelling tests – A critical review”. In: *Energy Procedia* 76 (2015). European Geosciences Union General Assembly 2015 - Division Energy, Resources and Environment, EGU 2015, pp. 96–105. DOI: https://doi.org/10.1016/j.egypro.2015.07.857.

[22] S Banu Ikizler et al. “Prediction of swelling pressures of expansive soils using soft computing methods”. In: *Neural Computing and Applications* 24.2 (Feb. 2014), pp. 473–485.

[23] Ramakrishna Bag et al. “Comparative study between MLR and ANN techniques to predict swelling pressure of expansive clays”. In: *Geotechnical and Geological Engineering* 40.7 (July 2022), pp. 3443–3455. DOI: 10.1007/s10706-022-02099-5.

[24] Yousif Ismael Mawlood et al. “Large-Scale Model Swelling Potential of Expansive Soils in Comparison with Oedometer Swelling Methods”. In: *Iranian Journal of Science and Technology, Transactions of Civil Engineering* 44.4 (Dec. 2020), pp. 1283–1293.

[25] N. V. Nayak et al. “Swelling Characteristics of Compacted, Expansive Soils”. In: *Clays and Clay Minerals* 19.4 (Aug. 1971), pp. 251–261. DOI: 10.1346/CCMN.1971.0190406.

[26] H. B. Seed et al. “Prediction of Swelling Potential for Compacted Clays”. In: *Journal of the Soil Mechanics and Foundations Division* 88.3 (1962), pp. 53–87. DOI: 10.1061/JSFEAQ.0000431.

[27] Adnan A. Basma. “Prediction of Expansion Degree for Natural Compacted Clays”. In: *Geotechnical Testing Journal* 16 (1993), pp. 542–549. DOI: 10.1520/GTJ10294J.

[28] GF Sowers et al. “High volume change clays of the South-Eastern coastal plain”. In: *Proc. 3rd Pan Am. Conf. Soil Mechanics Foundation Engng*. 1967, pp. 99–120.

[29] BV Ranganatham et al. “A rational method of predicting swelling potential for compacted expansive clays”. In: *Proceedings of the 6th International Conference on Soils Mechanics and Foundation Engineering, Montreal*. 1965, pp. 92–96.

[30] Raymond Nen Yong et al. *Introduction to soil behavior*. Tech. rep. 1966.

[31] Charles L Nalezny et al. “Effect of soil structure and thixotropic hardening on swelling behavior of compacted clay soils”. In: *Highway Research Record* 209 (1967).

[32] Magdi Zumrawi. “Prediction of Swelling Characteristics of Expansive Soils”. In: *Journal of Sudan Engineering Society (JSES)* 58 (Sept. 2012), pp. 55–62.

[33] Chongzhi Qiao et al. “Enhancing gas solubility in nanopores: A combined study using classical density functional theory and machine learning”. In: *Langmuir* 36.29 (July 2020), pp. 8527–8536. ISSN: 0743-7463. DOI: 10.1021/acs.langmuir.0c01160.

[34] Changxi Huang et al. “Factors Affecting the Swelling-Compression Characteristics of Clays in Yichang, China”. In: *Advances in Civil Engineering* 2019 (Feb. 2019), p. 13.

[35] John Nelson et al. “A Case History of Structures Constructed on Expansive Soils”. In: Oct. 2019.

[36] Arindam Das et al. “Effect of expansive soil on foundation and its remedies”. In: *vol* 3 (2014), pp. 92–95.

[37] Sridharan, A. and Prakash, K. “Classification procedures for expansive soils”. In: *Proceedings of the Institution of Civil Engineers - Geotechnical Engineering* 143.4 (2000), pp. 235–240. DOI: 10.1680/geng.2000.143.4.235.

[38] Stephen Hillier. “Clay mineralogy”. In: Jan. 1978, pp. 223–228. DOI: 10.1007/3-540-31079-7_47.

[39] Mohammed Fattah et al. “Swelling Behavior of Unsaturated Expansive Soil”. In: *Transportation Infrastructure Geotechnology* 8 (Mar. 2021). DOI: 10.1007/s40515-020-00112-z.

[40] Bojana Dolinar. “Predicting the normalized, undrained shear strength of saturated fine-grained soils using plasticity-value correlations”. In: *Applied Clay Science* 47.3 (2010), pp. 428–432. DOI: 10.1016/j.clay.2009.12.013.

[41] Brendan C. O’Kelly. “Briefing: Atterberg limits and peat”. In: *Environmental Geotechnics* 3.6 (2016), pp. 359–363. DOI: 10.1680/envgeo.15.00003.

[42] Hamish Cresswell et al. “Bulk density and pore space relations”. In: *Soil physical measurement and interpretation for land evaluation* (2002), pp. 35–58.

[43] Valéry Ferber et al. “On the swelling potential of compacted high plasticity clays”. In: *Engineering Geology* 104.3 (2009), pp. 200–210. DOI: doi.org/10.1016/j.enggeo.2008.10.008.

[44] Bertrand Teodosio et al. “A review and comparison of design methods for raft substructures on expansive soils”. In: *Journal of Building Engineering* 41 (2021), p. 102737. DOI: 10.1016/j.jobe.2021.102737.

[45] Scott Gould et al. “A void ratio - water content - net stress model for environmentally stabilized expansive soils”. In: *Canadian Geotechnical Journal* 48.6 (2011), pp. 867–877. DOI: 10.1139/t10-108.

[46] Amir Modarres et al. “Clay stabilization using coal waste and lime — Technical and environmental impacts”. In: *Applied Clay Science* 116-117 (2015), pp. 281–288. DOI: https://doi.org/10.1016/j.clay.2015.03.026.

[47] Işık Yilmaz et al. “Multiple regression, ANN (RBF, MLP) and ANFIS models for prediction of swell potential of clayey soils”. In: *Expert Systems with Applications* 38.5 (May 2011), pp. 5958–5966. ISSN: 0957-4174. DOI: 10.1016/j.eswa.2010.11.027.

[48] Birhanu Ermias et al. “Application of Artificial Intelligence for Prediction of Swelling Potential of Clay-Rich Soils”. In: *Geotechnical and Geological Engineering* 38.6 (Dec. 2020), pp. 6189–6205. ISSN: 1573-1529. DOI: 10.1007/s10706-020-01427-x.

[49] E. U. Eyo et al. “Improved prediction of clay soil expansion using machine learning algorithms and meta-heuristic dichotomous ensemble classifiers”. In: *Geoscience Frontiers* 13.1 (Jan. 2022), p. 101296. ISSN: 1674-9871.

[50] Yusuf Erzin et al. *The Prediction of Swell Percent and Swell Pressure by Using Neural Networks*. 2011. DOI: 10.3390/mca16020425.

[51] Iman Ashayeri et al. “Free-Swell and Swelling Pressure of Unsaturated Compacted Clays; Experiments and Neural Networks Modeling”. In: *Geotechnical and Geological Engineering* 27.1 (May 2008), p. 137. DOI: 10.1007/s10706-008-9219-y.

[52] C. Kayadelen et al. “Adaptive neuro-fuzzy modeling for the swelling potential of compacted soils”. In: *Environmental Earth Sciences* 59.1 (Feb. 2009), p. 109. ISSN: 1866-6299. DOI: 10.1007/s12665-009-0009-5.

[53] ADNAN A. BASMA et al. “Modeling Time Dependent Swell of Clays Using Sequential Artificial Neural Networks”. In: *Environmental & Engineering Geoscience* 9.3 (Mar. 2003), pp. 279–288. ISSN: 1078-7275. DOI: 10.2113/9.3.279.

[54] Janardhan Tahasildar et al. “Development of relationships between swelling and suction properties of expansive soils”. In: *International Journal of Geotechnical Engineering* 12.1 (2018), pp. 53–65. DOI: 10.1080/19386362.2016.1250040.

[55] Sarat Kumar Das et al. “Prediction of swelling pressure of soil using artificial intelligence techniques”. In: *Environmental Earth Sciences* 61.2 (July 2010), pp. 393–403. DOI: 10.1007/s12665-009-0352-6.

[56] S. Banu Ikizler et al. “Prediction of swelling pressures of expansive soils using artificial neural networks”. In: *Advances in Engineering Software* 41.4 (2010), pp. 647–655. DOI: https://doi.org/10.1016/j.advengsoft.2009.12.005.

[57] A. Surgel. “A Survey of The Geotechnical Properties of Ankara Soils”. M.S. Thesis. METU Civil Engineering Department, 1976, 96 Pages.

[58] Donald R. Snethen et al. *An Evaluation of Expedient Methodology for Identification of Potentially Expansive Soils*. English. FHWA-RD-77-94. June 1977.

[59] Erdal Çokça. “Swelling potential of expansive soils with a critical appraisal of the identification of swelling of Ankara soils by methylene blue tests”. PhD thesis. Middle East Technical University, 1991.

[60] E. Çokça. “Relationship between methylene blue value, initial soil suction and swell percent of expansive soils”. In: *Turkish Journal of Engineering and Environmental Sciences* 26 (Jan. 2002), pp. 521–529.

[61] Ömür Çimen et al. “Prediction of Swelling Potential and Pressure in Compacted Clay”. In: *Arabian Journal for Science and Engineering* 37.6 (Sept. 2012), pp. 1535–1546. ISSN: 2191-4281. DOI: 10.1007/s13369-012-0268-4.

[62] Yusuf Erzin et al. “The unique relationship between swell percent and swell pressure of compacted clays”. In: *Bulletin of Engineering Geology and the Environment* 72.1 (Feb. 2013), pp. 71–80. ISSN: 1435-9537. DOI: 10.1007/s10064-013-0461-z.

[63] Bader A. Hakami et al. “Expansive potentiality of sabkha soils of Rabigh Lagoon, Saudi Arabia: a case study”. In: *Arabian Journal of Geosciences* 12.4 (Feb. 2019), p. 107. ISSN: 1866-7538. DOI: 10.1007/s12517-019-4271-x.

[64] A.S. Rao et al. “Prediction of swelling characteristics of remoulded and compacted expansive soils using free swell index”. In: *Quarterly Journal of Engineering Geology and Hydrogeology* 37.3 (Aug. 2004), pp. 217–226. ISSN: 1470-9236. DOI: 10.1144/1470-9236/03-052.

[65] Victor N. Kaliakin. “Chapter 2 - Example problems related to soil identification and classification”. In: *Soil Mechanics*. Ed. by Victor N. Kaliakin. Butterworth-Heinemann, 2017, pp. 51–92. DOI: https://doi.org/10.1016/B978-0-12-804491-9.00002-1.

[66] M. Tonoz et al. “A laboratory-scale experimental investigation on the performance of lime columns in expansive Ankara (Turkey) Clay”. In: *Bulletin of Engineering Geology and the Environment* 62.2 (May 2003), pp. 91–106. DOI: 10.1007/s10064-002-0176-z.

[67] Kamil Kayabali et al. “Measurement of swelling pressure: direct method versus indirect methods”. In: *Canadian Geotechnical Journal* 48.3 (2011), pp. 354–364. DOI: 10.1139/T10-074.

[68] Jiro Doke. *GRABIT*. 2022. URL: https://www.mathworks.com/matlabcentral/fileexchange/7173-grabit. MATLAB Central File Exchange. Retrieved July 19, 2022.

[69] Kurt Hornik et al. “Multilayer feedforward networks are universal approximators”. In: *Neural Networks* 2.5 (1989), pp. 359–366. ISSN: 0893-6080. DOI: https://doi.org/10.1016/0893-6080(89)90020-8.

[70] Varun Kumar Ojha et al. “Metaheuristic design of feedforward neural networks: A review of two decades of research”. In: *Engineering Applications of Artificial Intelligence* 60 (2017), pp. 97–116. ISSN: 0952-1976. DOI: https://doi.org/10.1016/j.engappai.2017.01.013.

[71] Reza Taherdangkoo et al. “Modeling Solubility of Anhydrite and Gypsum in Aqueous Solutions: Implications for Swelling of Clay-Sulfate Rocks”. In: *Rock Mechanics and Rock Engineering* (Apr. 2022). ISSN: 1434-453X. DOI: 10.1007/s00603-022-02872-1.

[72] Tamal Ghosh et al. “CFNN-PSO: An Iterative Predictive Model for Generic Parametric Design of Machining Processes”. In: *Applied Artificial Intelligence* 33.11 (Sept. 2019), pp. 951–978. ISSN: 0883-9514. DOI: 10.1080/08839514.2019.1661110.

[73] Budi Warsito et al. “Cascade Forward Neural Network for Time Series Prediction”. In: *Journal of Physics: Conference Series* 1025 (May 2018), p. 012097. DOI: 10.1088/1742-6596/1025/1/012097.

[74] Omaima N. Ahmad AL-Allaf. “Cascade-forward vs. function fitting neural network for improving image quality and learning time in image compression system”. In: *Lecture Notes in Engineering and Computer Science* 2 (2012), p. 7. ISSN: 2078-0958.

[75] Sumit Goyal et al. “Cascade and feedforward backpropagation artificial intelligence models for prediction of sensory quality of instant coffee flavoured sterilized drink”. In: *Canadian Journal on Artificial Intelligence, Machine Learning and Pattern Recognition* 79–82 (Aug. 2011), p. 17.

[76] P.G. Benardos et al. “Optimizing feedforward artificial neural network architecture”. In: *Engineering Applications of Artificial Intelligence* 20.3 (2007), pp. 365–382. DOI: 10.1016/j.engappai.2006.06.005.

[77] Frank Burden et al. “Bayesian Regularization of Neural Networks”. In: *Artificial Neural Networks: Methods and Applications*. Ed. by David J. Livingstone. Totowa, NJ: Humana Press, 2009, pp. 23–42. DOI: 10.1007/978-1-60327-101-1_3.

[78] M.T. Hagan et al. “Training feedforward networks with the Marquardt algorithm”. In: *IEEE Transactions on Neural Networks* 5.6 (1994), pp. 989–993. DOI: 10.1109/72.329697.

[79] Donald W. Marquardt. “An Algorithm for Least-Squares Estimation of Nonlinear Parameters”. In: *Journal of the Society for Industrial and Applied Mathematics* 11.2 (June 1963), pp. 431–441. DOI: 10.1137/0111030.

[80] Peter J. Rousseeuw et al. “Outlier Diagnostics”. In: *Robust Regression and Outlier Detection*. John Wiley ‘I&’ Sons, Ltd, 1987, pp. 216–247. DOI: 10.1002/0471725382.ch6.

[81] Reza Taherdangkoo et al. “Gaussian process regression to determine water content of methane: Application to methane transport modeling”. In: *Journal of Contaminant Hydrology* 243 (2021), p. 103910. ISSN: 0169-7722. DOI: https://doi.org/10.1016/j.jconhyd.2021.103910.

[82] Reza Taherdangkoo et al. “Predicting methane solubility in water and seawater by machine learning algorithms: Application to methane transport modeling”. In: *Journal of Contaminant Hydrology* 242 (2021), p. 103844. ISSN: 0169-7722. DOI: https://doi.org/10.1016/j.jconhyd.2021.103844.

[83] David C. Hoaglin et al. “The Hat Matrix in Regression and ANOVA”. In: *The American Statistician* 32.1 (1978), pp. 17–22. DOI: 10.1080/00031305.1978.10479237.

[84] Amir H. Mohammadi et al. “A novel method for evaluation of asphaltene precipitation titration data”. In: *Chemical Engineering Science* 78 (2012), pp. 181–185. DOI: 10.1016/j.ces.2012.05.009.

[85] Zeynal Abiddin Erguler et al. “A simple test and predictive models for assessing swell potential of Ankara (Turkey) Clay”. In: *Engineering Geology* 67.3 (2003), pp. 331–352. DOI: https://doi.org/10.1016/S0013-7952(02)00205-3.

[86] Victor Cantillo et al. “Empirical correlations for the swelling pressure of expansive clays in the city of Barranquilla, Colombia”. In: *Earth Sciences Research Journal* 21.1 (June 2017), pp. 45–49. DOI: 10.15446/esrj.v21n1.60226.

[87] Xiong Wu et al. “The relationship between the swelling pressure and shear strength of unsaturated soil: the Yanji Basin as a case study”. In: *Arabian Journal of Geosciencesa* 10.15 (Aug. 2017), p. 330.

[88] Reza Taherdangkoo et al. “Nonlinear Autoregressive Neural Networks to Predict Hydraulic Fracturing Fluid Leakage into Shallow Groundwater”. In: *Water* 12.3 (2020). DOI: 10.3390/w12030841.